THE DEVELOPMENT OF AN ENERGY MONITORING SYSTEM FOR THE ASSESSMENT OF VARIABILITY IN PROCTOR COMPACTION RESULTS

By

KEITH BERISWILL

A THESIS PRESENTED TO THE GRADUATE SCHOOL
OF THE UNIVERSITY OF FLORIDA IN PARTIAL FULFILLMENT
OF THE REQUIREMENTS FOR THE DEGREE OF
MASTER OF ENGINEERING

UNIVERSITY OF FLORIDA

2009

© 2009 Keith Beriswill

To Rebecca

ACKNOWLEDGMENTS

I thank all of the people that have been there for me throughout the difficult times associated with pursuing higher education, as well as for all of the encouragement that I have received over the years from those close to me. I would especially like to thank my parents, grandparents and my bride-to-be.

I would like to thank Jeff Beriswill for being such a wonderful role model and for introducing me to Civil and Geotechnical Engineering.

Scott Wasman, Dr. McVay and Dr. Bloomquist, thank you so much for all of your time effort and willingness to share your knowledge. Chuck Broward and George Lopp, I thank you for your time, skill and tools.

TABLE OF CONTENTS

page

LIST OF TABLES

LIST OF FIGURES

Abstract of Thesis Presented to the Graduate School
of the University of Florida in Partial Fulfillment of the
Requirements for the Degree of Master of Engineering

THE DEVELOPMENT OF AN ENERGY MONITORING SYSTEM FOR THE ASSESSMENT OF VARIABILITY IN PROCTOR COMPACTION RESULTS

By

Keith Beriswill

May 2009

Chair: David Bloomquist
Co chair: Michael McVay
Major: Civil Engineering

Existing techniques used to calibrate soil compaction equipment do not measure the overall imparted energy into the soil. Instead, various parameters (i.e., drop height, rammer mass, etc.) are measured independently and hence one is forced to assume that the theoretical energy is mobilized. Since the results of the Proctor density tests are critical to field compaction control, a calibration system is needed to ensure consistency in the equipment used by the Florida Department of Transportation (FDOT), consultant, and contractor testing labs.

A new portable calibration device has been developed that measures rammer speed and base system forces during impact, and outputs the kinetic of the rammer and base compliance energy of the compaction machine. The calibrator was used to test 30 compactors in the state of Florida. However, there was a trend indicating a lower than acceptable available energy for compaction.

Soil density pills were then compacted on several of the machines and the results used to determine a linear regression equation for two target moisture contents in order to describe the effect of the variables on resulting dry density. The variances associated with each of the

dependent variables were then used to account for variance observed in the population of dry density results.

The results of this study will be used by labs to check and adjust their equipment so that results from disparate labs can be used with increased confidence. FDOT's Independent Assurance Inspection teams will also be able to provide a performance-based check.

CHAPTER 1
INTRODUCTION

1.1 Background

The Florida Department of Transportation (FDOT) and many other entities rely on the compaction of soil for infrastructure construction projects. This requires that a sample of onsite soils be compacted in a laboratory, in order to establish the requirements for field compaction. Explicitly, the characteristics of interest are the maximum dry unit weight and the optimum moisture content of the particular soil. Whether the test is being performed by the FDOT or by a private consulting laboratory, the testing procedure remains unchanged.

The Proctor compaction test consists of two primary types of tests; the Standard American Association of State Highway Transportation Officials (AASHTO) Standard T-99 and the Modified AASHTO T-180 test. For each test, a rammer of a specified size, shape and mass is lifted to a specified height and allowed to fall until reaching a soil sample. The material is contained in a mold of specified size for a set number of impacts per soil lift. As a result of the rammer impact, compaction or densification of the soil occurs and should be directly related to the amount of energy that is produced. For a given compaction test, the amount of total energy that is delivered to a volume of soil is:

$$E = \frac{\begin{pmatrix}\text{number of}\\ \text{blows per}\\ \text{layer}\end{pmatrix} \times \begin{pmatrix}\text{number}\\ \text{of}\\ \text{layers}\end{pmatrix} \times \begin{pmatrix}\text{weight}\\ \text{of}\\ \text{hammer}\end{pmatrix} \times \begin{pmatrix}\text{height of}\\ \text{drop of}\\ \text{hammer}\end{pmatrix}}{\text{volume of mold}} \qquad (1\text{-}1)$$

With an increase in applied energy, an increase in dry density will likely occur if the soil moisture content is maintained (Proctor 1933). Additionally, the optimum moisture content of the soil will vary for different amounts of energy imparted to the soil (Dubose 1952). This dependency of maximum dry unit weight and moisture content on energy is illustrated in Figure

1-1. Due to the effect of compaction energy on the resulting densities, it is critical that the energy and testing procedure be consistent. In this illustration, mass and drop height remained constant while the number of blows per layer increase and is representative of adding energy imparted to the soil.

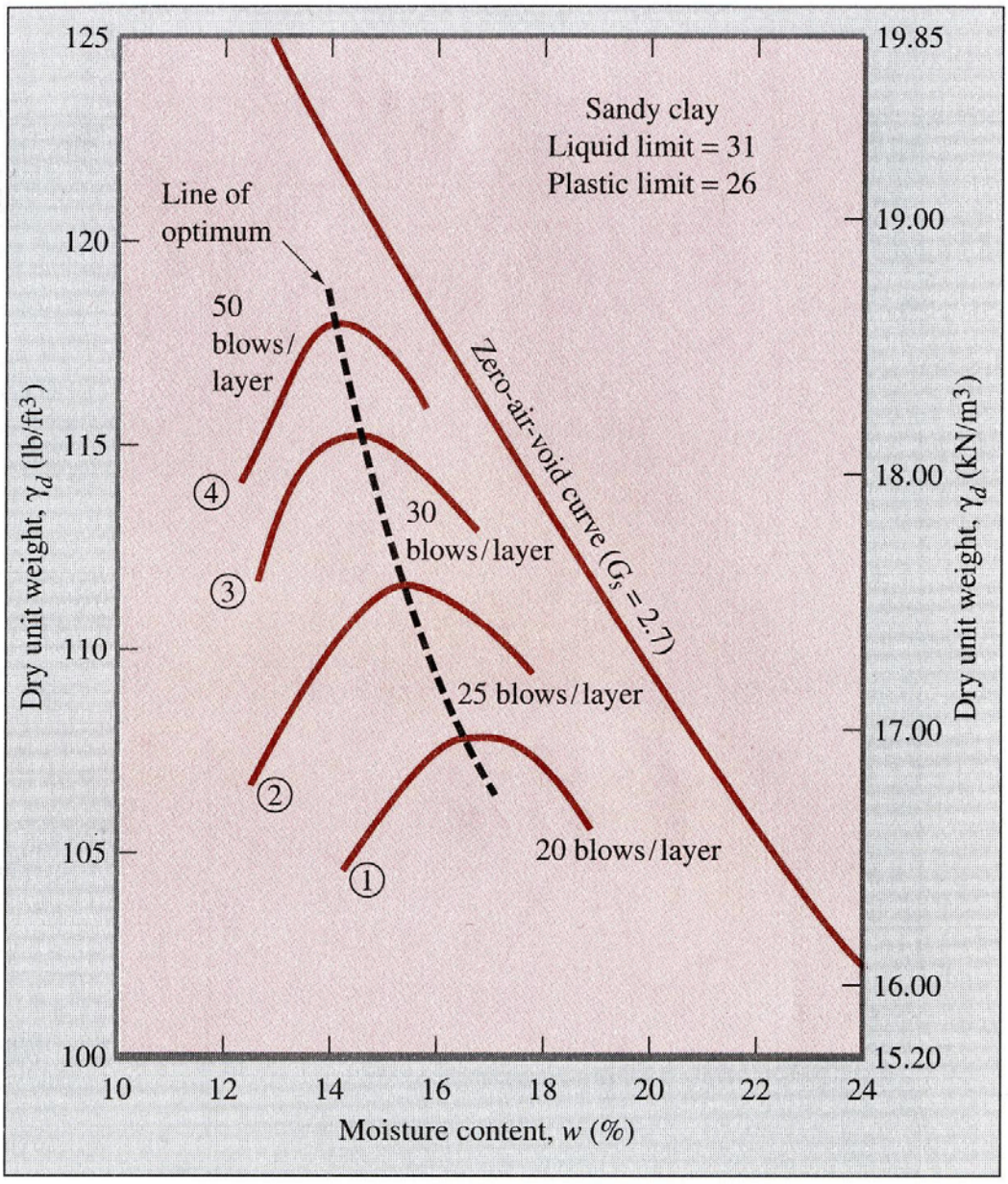

Figure 1-1. Effect of compaction energy on compaction of sandy clay (Das 2002).

In an effort to verify that mechanical compaction machines are delivering the prescribed energy, a calibration procedure is periodically performed. One calibration method, specified by AASHTO, is based on the deformation a lead cylinder upon rammer impact (ASTM D 2168 B). However, the method used by the FDOT utilizes the compaction of a calibration clay (CL) material as prescribed by ASTM D 2168 A. For this method, the CL material is compacted using a manual Proctor compactor and the results compared to a specific machine to be calibrated (AASHTO T-99 or T-180). Utilizing the manual testing procedure, the maximum dry unit weight and optimum moisture content of the soil are determined. It is then performed using the mechanical method (AASHTO T-99 or T-180) and the maximum dry unit weight compared. Attention is focused on the percent difference between the two maximum dry unit weights. When the absolute percent difference between the maximum dry unit weights for the two testing procedures is less than 2%, the mechanical calibrator is considered to be calibrated.

1.2 Problem Statement

In previous work performed by the FDOT, large quantities of soil were obtained, divided, and sent to state-approved private testing laboratories that use compaction machines calibrated via AASHTO D 2168 A. These samples were then tested in accordance with AASHTO specifications for the AASHTO T-99 Standard and AASHTO T-180 Modified testing procedures. The results from this testing regime displayed differences in the maximum dry densities and optimum moisture content reported from lab to lab. There appear to be two primary possibilities for these differences. Since the same soil was used for all testing, the possibility of soil properties skewing the results was assumed to be negligible. Thus, it was hypothesized there is some difference in the compactive energies across labs, or the operator had an effect on the results.

While the energy applied to the soil specimen is known to have a pronounced effect on density, it is not the only factor that needs to be considered. Base support can play a critical effect on both density and optimum moisture content (Chapman and Ray 1954). Knowing that different base conditions do exist between laboratories, this research was launched to investigate both energy delivery and energy dissipation on resulting densities.

1.3 Objective and Scope of Work

As a result of the discrepancies in the maximum dry unit weight and optimum moisture content, the primary goal of this research was to take an energy based approach to the calibration of mechanical soil compactors. This involved being able to measure the energy available for compaction and the energy transferred to the base (base compliance) of the compaction machine. A portable calibration device was developed which measures both the rammer impact velocity and base system energy. It was then tested throughout FDOT district compaction laboratories.

The construction and validation of the device was performed at the Department of Civil and Coastal Engineering Laboratory at the University of Florida (UF) in Gainesville. Tests in several districts were performed on a population of thirty machines - mostly as AASHTO D T-180 Modified compactors. The results were compiled and analyzed to establish a confident variance in energy available for compaction and base system energy. As components of the compaction process, these two quantifiable values comprise two-thirds of it, with the variance of the operator involving such things as moisture control, layer thickness, particle distribution, pre-tamping, and moisture determination. This issue was only identified as a contributor in soil density variance, as the time required for a testing was not available.

The scope of work found that the variance in compaction energy was half the variance in the base system energy. Although the compaction variance was small indicating similarity among machines in the test population, the mean energy was less than that prescribed by

AASHTO T-180 and ASTM D 1557 Standards. The difference is attributed to machine performance due to drop height and impact velocity, and not on the mass of the rammer. Variance in base system energy is attributed to the many different base foundations discovered in the population. Typically, foundations consisted of some form of concrete, either cast or constructed with concrete blocks, and cemented in place.

Soil density tests were performed on A-2-4 soil samples on machines tested with the developed energy devices. The results of these density tests in conjunction with the measured energies of the machines were used to develop regression equations that describe the interactions of the dependant variables on the resulting dry densities. These regression equations were then used to quantify the variance projected from the variability observed in the dependent variables. This was able to attribute half of the observed variance in dry density to the variance observed in, moisture content, dry density and base compliance.

CHAPTER 2
BACKGROUND

2.1 Mechanics of Compaction

Soil compaction is performed for the purpose of increasing the strength of the soil through densification (Proctor 1933). The process by which this increased density is reached is through the removal of air voids between soil particles (Das 2002). With the removal of the air voids, it is possible to increase the mass of soil in a finite volume. In order to most efficiently remove air, water is added allowing the soil particles to slide past one another as mechanical energy is applied. When the same amount of energy is applied and the amount of water is increased, eventually a maximum mass of soil will result. From this point on, the addition of water will serve to displace soil particles resulting in decreased density (Figure 2-1).

2.2 Delivered Energy and Soil Compaction

The energy that an object possesses in free fall is the sum of its potential and kinetic energy (Equation 2-1). In this situation it can be assumed that the instant the rammer is at its apogee, its velocity is zero. Thus, the rammer possesses only potential energy and its kinetic energy is zero (Equation 2-2). This case is opposite at the instant that the hammer has fallen and just prior to impact. Here, the object has no potential energy but possesses only kinetic energy (Equation 2-3) (Halliday 2000).

$$\text{Total energy} = (\tfrac{1}{2} \text{ mass} \times \text{velocity}^2) + (\text{mass} \times \text{gravity} \times \text{height}) \quad (2\text{-}1)$$

$$\text{Energy at drop height} = (\text{mass} \times \text{gravity} \times \text{height}) \quad (2\text{-}2)$$

$$\text{Energy at impact} = (\tfrac{1}{2} \text{ mass} \times \text{velocity}^2) \quad (2\text{-}3)$$

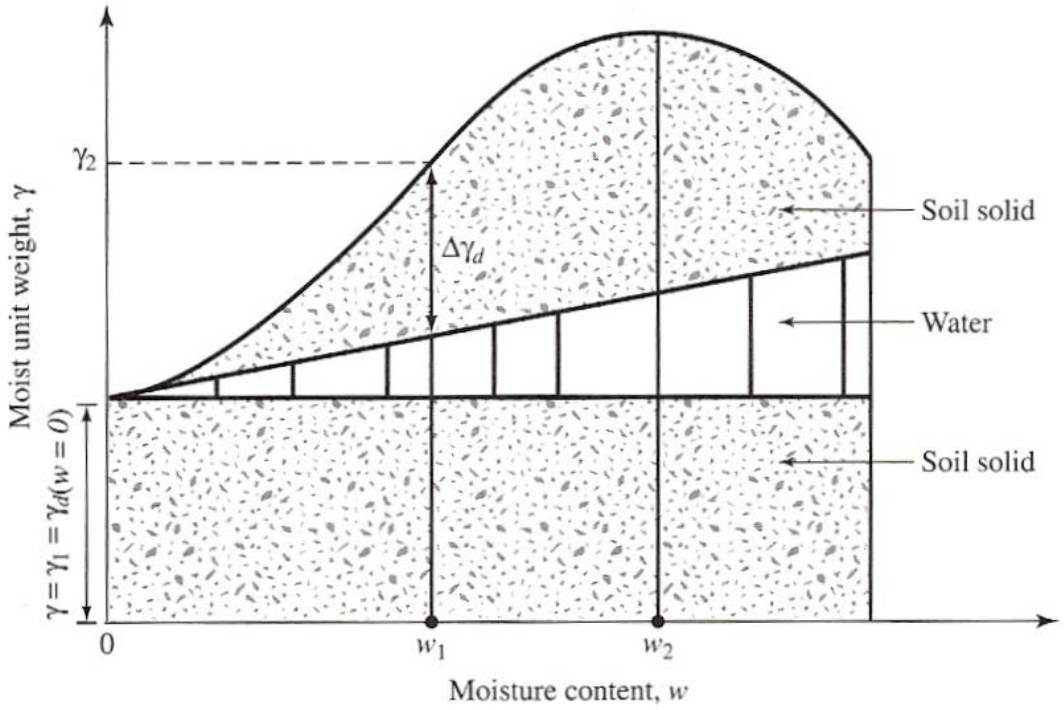

Figure 2-1. Effect of moisture content on dry density (Das 2002).

Based on conservation of energy, if the loss due to friction is negligible, then the energy at the drop height is equivalent to the energy at the instant of impact. The drop height and mass are each specified in AASHTO, and once verified to be within tolerance, the velocities for the T-99 and T-180 tests can be calculated through simple algebra.

AASHTO T-99 calls for a 5.5-lb rammer to be dropped 12 inches, thus producing 5.5 ft-lb of energy each drop. The T-180 method calls for a 10-lb rammer to be dropped 18 inches, resulting in a theoretical energy of 15 ft-lb being delivered (neglecting friction). AASHTO does however make allowance for differences in the drop height mass of the rammer for both testing procedures. This is ± 0.06 inches and ± 0.02 lb, respectively. Assuming the reduction in energy is negligibly affected by friction, for the Standard Proctor compaction test this results in a range of acceptable energy of 5.45 to 5.55 ft-lb. For the Modified Proctor compaction tests, the range is 14.92 to 15.08 ft-lb.

2.3 Previous Research on Energy Measurement

The Transportation Research Board (TRB) has published research that took an energy based approach to monitoring the compaction process. It also used the technique for soil compactor calibration (Sebesta and Liu 2007). Sebesta and Liu's research focused on a permanently mounted displacement sensor that utilized a magneto-restrictive rod and sensing ring concentrically mounted above the rammer rod.

While this method may be used in a particular lab to measure the impact velocity of a rammer, it does not appear that it lends itself for use on multiple machines in other labs, nor could it be used to establish the energy delivered from a manual compaction hammer. The study proved useful in measuring impact velocity but proved to be ineffective as a portable energy calibrator due to the permanent mounting requirements of the displacement sensor.

Most critically, they found that successive impacts of a mechanical compaction rammer do not provide equal energy. This means that multiple successive impacts needed to be monitored.

2.4 Previous Research on the Variability of the Soil Compaction Process

Reproducibility of soil compaction has been previously investigated using a 2.5-kg and 4.5-kg (5.51-lb and 9.92-lb) rammer, comparable to the T-99 and T-180 testing procedures by British standards for both manual and mechanical compactors. According to The Roadway Research Laboratory, "No significant differences could be observed between the results achieved by hand compaction and those achieved by machine compaction" (Sherwood 1970). In terms of the observations made in this research, it was also noted that no faulty hand held rammers were observed in any laboratories and that the masses and drop heights of all handheld rammers were consistent. Thus, they concluded that differences in testing using the handheld rammer could only be documented by observing the actual test.

Of primary interest in their study was the effect a single operator had on soil density and optimum moisture content results, as well as the effect of different laboratories. Their results showed that an operator using the same machine to run multiple tests showed little variance, with a maximum dry density COV of 0.13 and 0.84 for optimum moisture content, whereas eight operators on a single machine had a maximum dry density COV of 2.8 and 7.8 for optimum moisture content for the same soil. The Road Research Laboratory then looked at results for 36 laboratories and found a COV of 2.1 for maximum dry density and 9.7 for moisture content. These results illustrate that the testing procedures of a single operator tend to be far more consistent than between individuals or different laboratories. The research did not seek to identify the source of the differences between the laboratory testing results in terms of the mechanical compaction equipment (Sherwood 1970).

2.5 Base Compliance

In UF research, an effort to determine the effect of a worse-case scenario regarding the base stiffness of a mechanical compactor was investigated. Two 0.75-inch thick plywood sheets were bolted to the top of a concrete compaction foundation block in the Soils Compaction Lab (Figure 2-2).

Six manual T-99A tests were then performed, two each on A-3, A-1-b and A-2-4 soils; one with and one without the plywood cushion. As expected, the boundary condition had a profound effect on the shape of the compaction curve as well the maximum dry density (Figure 2-3). The resulting density varied between 0.7% and 3.4% lower with the wood base compared to the T-99A standard procedure. For the A-3 soil, the optimum moisture content varied by more than 1%.

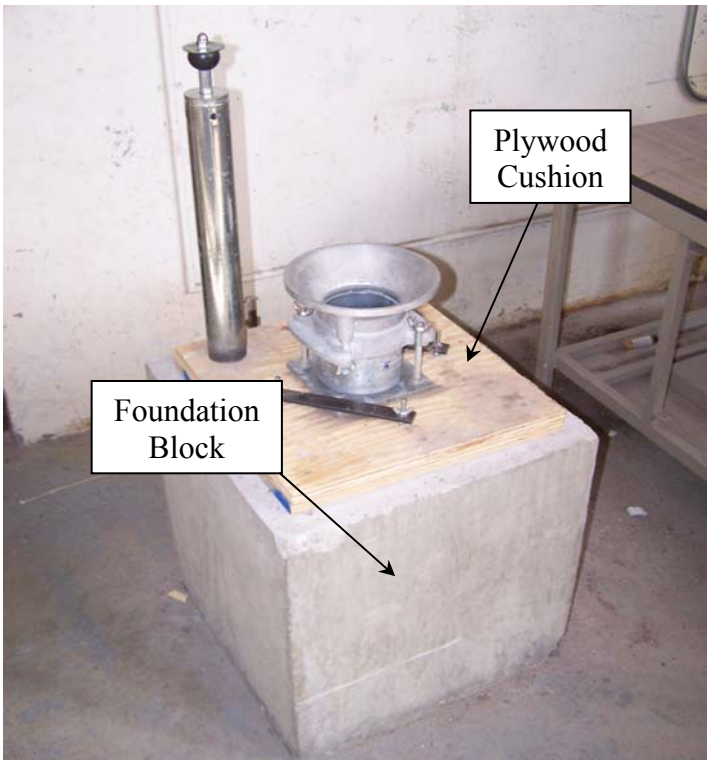

Figure 2-2. Compaction foundation block with wood cushion in place.

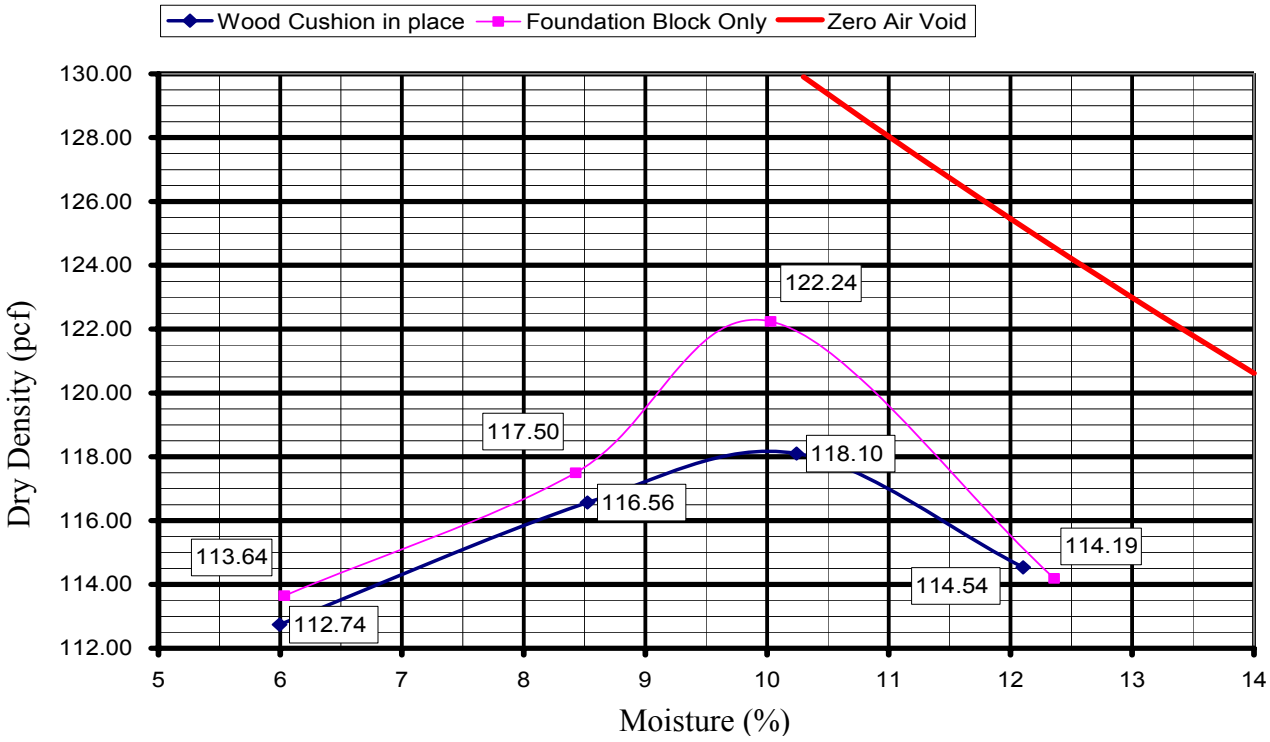

A

Figure 2-3. Effect of wood cushion on soil Proctor curve per soil type. A) Soil A-1-b. B) Soil A-3. C) Soil A-2-4.

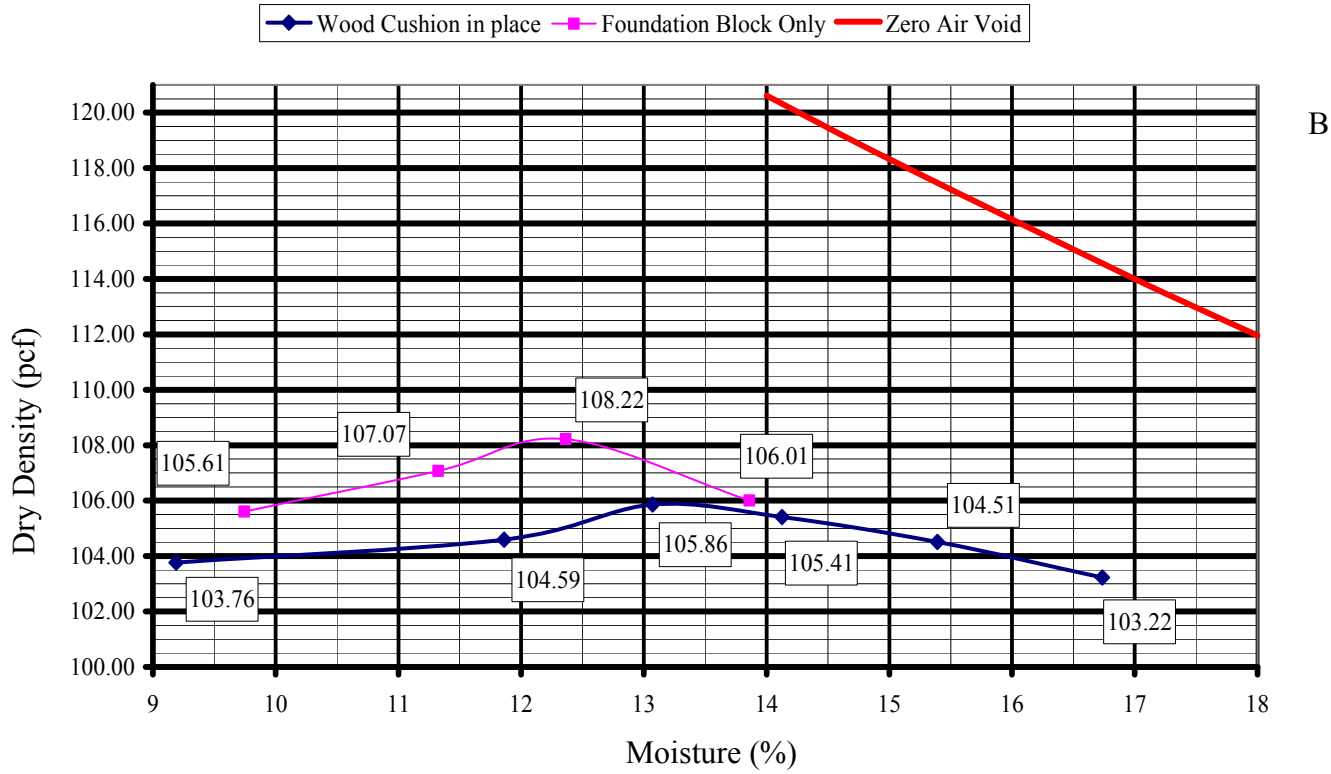

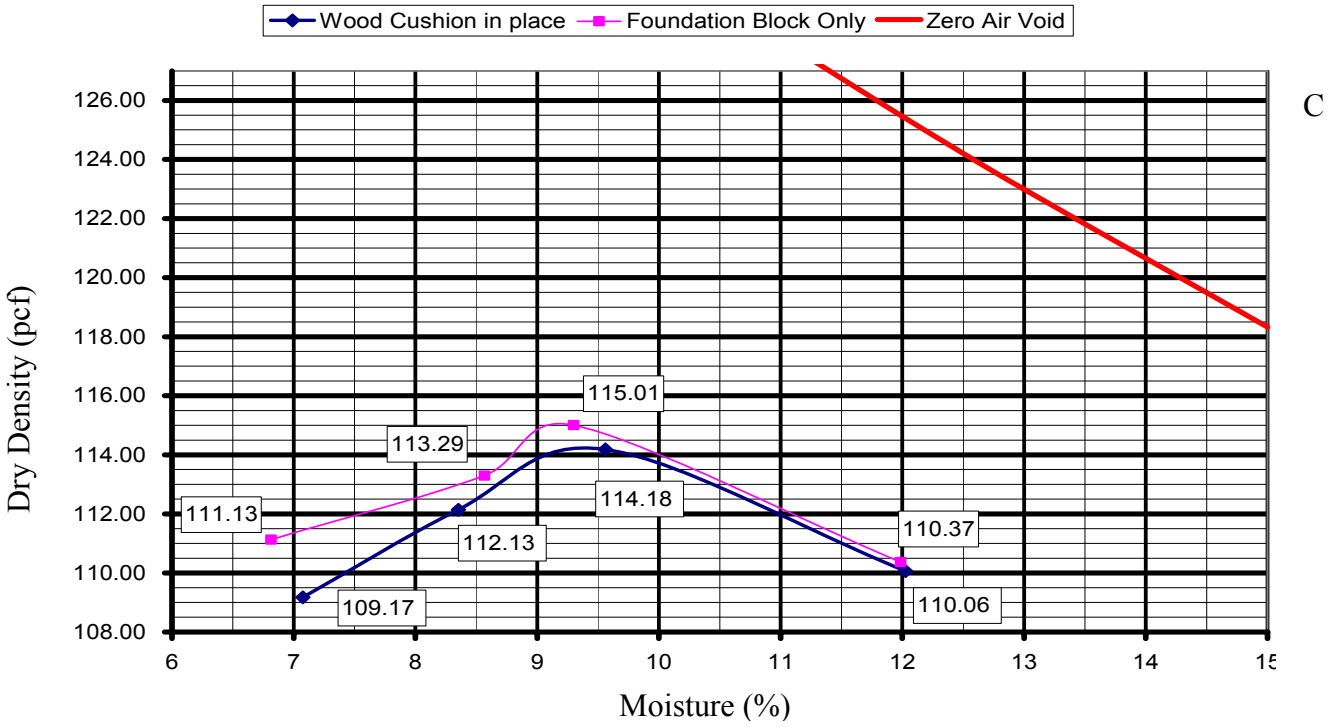

Figure 2-3. Continued.

2.6 Statistical Background

Statistical interpretation and representation of data is critical in the analysis of random variables. The variables contained within the topic of this research have been dealt with as statistically random variables, meaning they vary independently of each other. In most cases these variables have will be sampled a set number of times and summarized by their mean and variance (Equations 2-4 and 2-5)

$$\bar{x} = \frac{1}{n} \cdot \sum_{i=1}^{n} x_i \tag{2-4}$$

$\bar{x}$ = Mean of x
n = Number of Samples
x_i = Sample i

$$Var(x) = E\left[(x - \mu)^2\right] \tag{2-5}$$

$Var(x)$ = Variance of x
E = Expected Value
x = Sample
μ = Mean of x

In many cases it is necessary to verify that enough samples have been taken to establish accurately the variance. This calls for the use of a statistical method of inferring what the variance of the population is from the data obtained. The method for doing this that will be used is a method known as bootstrapping. This method of sampling useful because it does not require that the distribution of the data be know.

Bootstrapping is the term used for repetitive re-sampling of data. In order to perform a bootstrap only a sample of data is needed. From this sample of data a random value is selected a set number of times, the selected values are then summarized by their mean and variance to generate a single boot strap. This is then performed repetitively until the mean of the bootstrap

means and the variance of the bootstrap means reaches a constant value. These bootstraps are then considered representative of the population. Additional summary statistics can be then performed on the bootstraps to indicate if the enough samples were taken from the population. this is done by looking at the variance of the bootstrap variances, if enough samples from the population were originally acquired this value will be much smaller than the variance of the sample population. If too few samples from the population were taken the variance of the variance will be a large number.

Another method of determining if enough samples have been taken is to look at the coefficient of variation of the bootstrap variances. If this value exceeds a pre determined percentage then more samples should be acquired in order to accurately determine the variance of the sample population.

CHAPTER 3

THE CALIBRATION DEVICE

3.1 Operation of the Compaction Machine

The typical compaction machine used consulting labs in Florida as well as the FDOT's State Materials Office (SMO) is the Rainhardt Model 662 or similar machine (Figure 3-1). This machine consists of an electric motor that drives a belt which rotates a flywheel and attached cable to lift a grabber vertically. The lift height is a calibrated, controlled distance specific to the test, either 12 ± 0.06 inches or 18 ± 0.06 inches. This grabber travels along the rammer rod and grabs the rod at its lowest point of travel, rotates the rod a fixed increment during the lift and releases it at the highest point of travel at which time the rammer rod falls vertically. While falling, the rammer rod passes through the jaws of the grabber and is guided by a disk on the rammer assembly along guide rods until impact. Figure 3-1 illustrates the main components of the mechanical compactor.

3.2 Fundamentals of the Calibrator

Development of an energy based calibrator required that the energy delivered to a soil sample be quantified. In order to perform this task, several general issues needed to be addressed. First, the rammer should be allowed to rotate freely during the compaction procedure. Secondly, the calibration device should function without altering the compactor, thereby voiding its calibration. This would then require a recalibration per AASHTO specifications prior to being used. Thirdly, no attachments to the rammer or guide rods are possible, since attaching any part of a calibrator to the rammer changes the rammer mass, and thus, the kinetic impact energy.

Figure 3-1. Typical mechanical soil compactor.

Observation at FDOT approved compaction laboratories indicated that in some, height above the compaction device was limited to less than 18 inches from the ceiling. This would have required cutting a hole in the ceiling to utilize Sebesta and Liu's device and thus was not pursued further.

3.3 Conceptual Designs

Several design strategies were formulated on ways the energy of a rammer compaction blow could be measured or calculated. In theory, quantification is a simple physics problem involving potential and kinetic energy and work theory. Using basic assumptions about the operation of the machine, these three aspects are related and it was determined that the energy might be measured through displacement, acceleration or the work done at impact via a dynamic load cell.

3.3.1 Dynamic Impact Calibrator

Initial instrumentation development focused on the principle that the kinetic energy of the rammer fall was equal to the work done. When the rammer impacts the soil, work is done as the soil deforms, the amount based on the soil's modulus. From the force measured during the deformation, one is able to employ the relationship between deformation and work (Equation 3-1). Assuming negligible losses occur, the work calculated would be the same as the energy that was delivered by the rammer.

$$W = \int_{y_1}^{y_2} F(y)\,dy \tag{3-1}$$

In this equation, W is the work done on the sample, F is the force applied to the specimen, and y is the deformation (compression) of the soil mass.

By inserting a dynamic force sensor at the location of the rammer impact point and measuring the displacement of the rammer during impact, Equation 3-1 could be calculated. In order to dampen the blow to protect the dynamic force sensor from excessive force and to provide measurable impact deformations, a relatively soft impact pad with known material properties was used.

A Micro-epsilon displacement laser with and operating frequency of 2,500 samples per second (2.5 kS/s) and precision of 0.001 of an inch was purchased for the project. In addition, a PCB 200C20 quartz piezoelectric analog dynamic force sensor with a range of 50,000 lb was acquired. The testing procedure consisted of conducting tests utilizing this instrumentation on a manual compaction hammer with different types of polyurethane and neoprene pads as the surface material. A two-inch diameter metal ring was installed on the compactor hammer to provide a target for the laser to reflect from. A frame was constructed to mount the laser displacement sensor. In addition, the frame contained two cross members with C-clamps in order to maintain vertical alignment of the hammer during a drop (Figure 3-2).

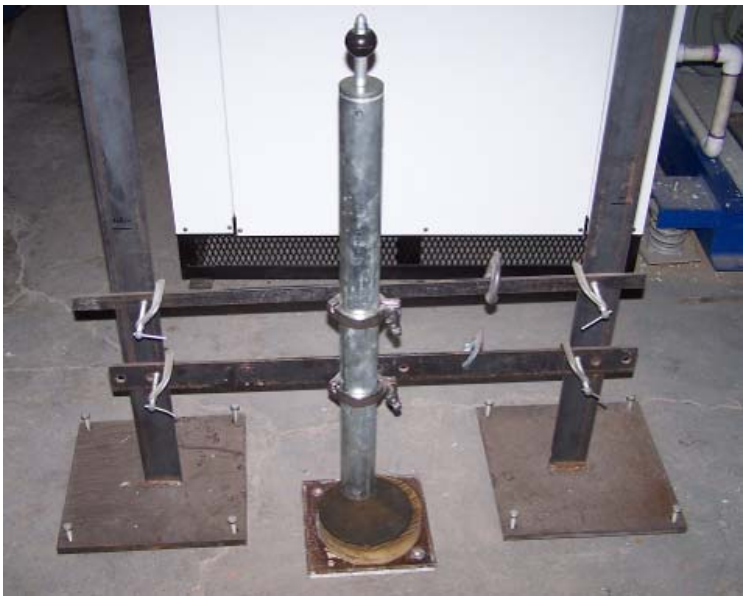

Figure 3-2. Manual rammer frame**.**

After several tests, this concept was abandoned since the hammer could not be moved around the mold as it would be during a compaction test run on mechanical compaction equipment. Based on this issue, allowing free rotation of the rammer became a high priority in the development of the calibration device.

3.3.2 Displacement Based Calibrator

Testing then focused on a displacement sensor that could measure the rammer's trajectory over its entire fall event. By utilizing an entire free fall set of data, the total displacement of the rammer for each impact could be determined (Equation 2-2, Section 2.2) and compared. However, more importantly, the impact velocity of the rammer also could be calculated and used to quantify the amount of kinetic energy that the rammer delivers with each impact (Equation 2-3, Section 2.2).

Using this knowledge and the goal of allowing free rotation of the rammer, testing began on the mechanical compactor. The mass of the rammer assembly was determined using a standard digital laboratory scale. A light (0.06-oz) metalized plastic disc target was affixed to the top of the rammer rod to serve as a target for the laser displacement sensor. The displacement transmitter/receiver was then mounted above the lift rod. Figure 3-3 illustrates the test setup. The full displacement record was then processed and analyzed to determine the total distance the rammer traveled over the course of the fall.

The displacements with respect to time were plotted and a second order trend line fitted through the data using Microsoft Excel. Refer to Figure 3-4 for a typical example of a plot.

Using the trend line for each of these displacement records, the first derivative was then taken with respect to time. This results in a velocity profile equation for the fall and was then evaluated at the time of impact, providing a calculated impact velocity of the rammer for each impact. The impact velocity was then used to evaluate the kinetic energy. The results of a series of rammer drops, fall distance, impact velocity, potential energy, and kinetic energy for each drop are presented in Table 3-1.

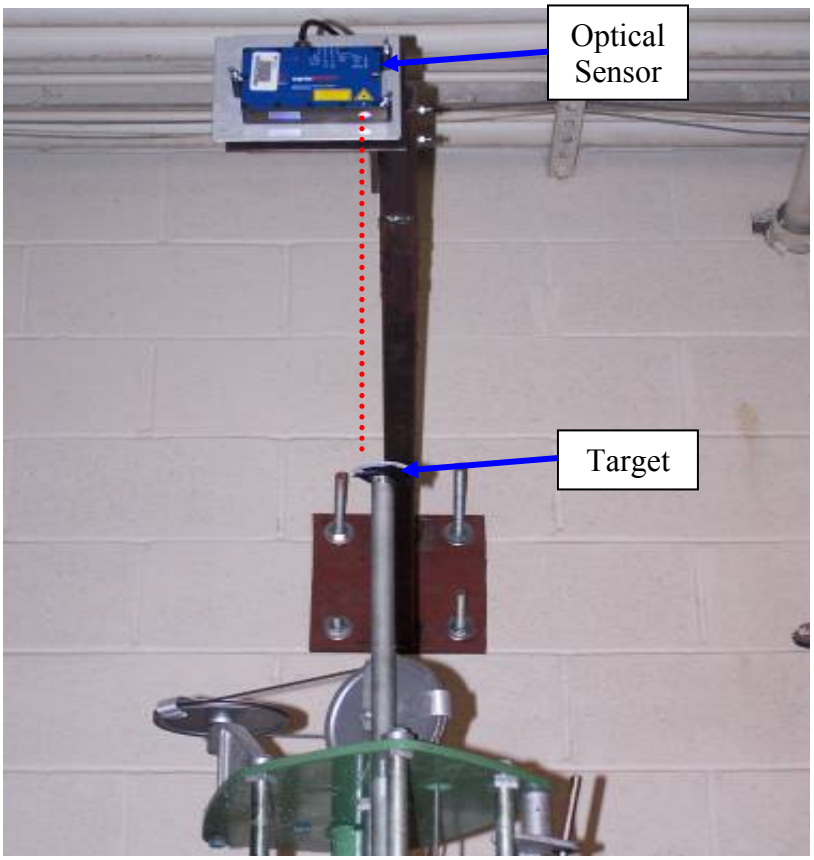

Figure 3-3. Compaction laboratory mechanical compactor displacement laser.

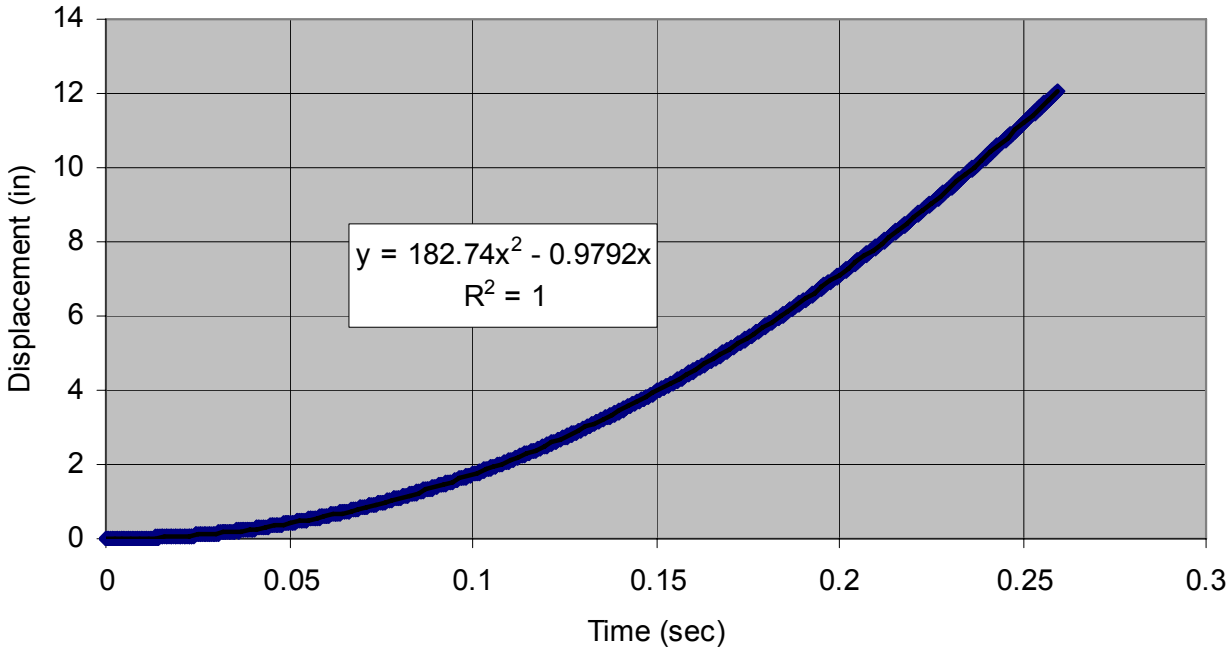

Figure 3-4. Laser recorded displacement versus time plot.

Table 3-1. Summary of Displacement Laser Energy Measurements (5.5-lb rammer)

Kinetic		Potential	
Velocity (ft/sec)	Energy (ft-lbs)	Displacement (in)	Energy (ft-lbs)
7.70	5.07	12.03	5.51
7.73	5.10	12.08	5.54
7.74	5.12	12.05	5.52
7.75	5.13	12.08	5.54
7.76	5.15	12.20	5.59
7.81	5.21	12.04	5.52
7.82	5.22	12.06	5.53
7.77	5.16	11.93	5.47
7.76	5.14	12.17	5.58
7.72	5.09	12.10	5.55

As expected, this table shows that in all cases, the kinetic energy is less than the potential energy. This is due to frictional losses from the rammer guide rods and disk contacting each other during free fall (Figure 3-5). It is important to note that the machine used at the UF compaction laboratory is not currently used for soil compaction but rather for prototype development and validation. Hence, it has not been certified as calibrated. However for calculation purposes, the mean drop height measured for these 10 impact was 12.07 inches which is very close to the tolerance of 0.06 inches specified in AASHTO standards.

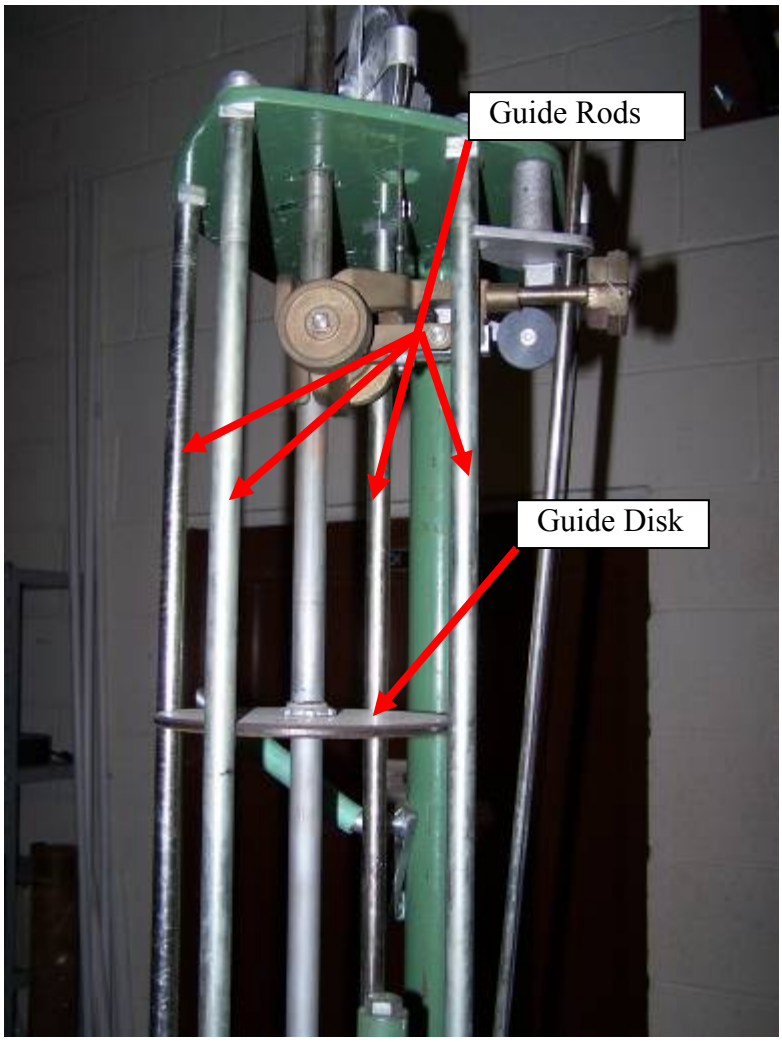

Figure 3-5. Detail of guide rods and guide disk.

These results verify that measuring the full rammer displacement during its fall may prove effective in accurately determining potential energy. Additionally, this study indicates there are significant differences in the actual versus theoretical kinetic energies, attributable to frictional losses. However, due to the mounting and clearance issues with the laser, its high cost and complexity of aligning the target with the laser, this concept was abandoned.

3.3.3 Acceleration Based Calibrator

The investigation then focused on using an accelerometer for determining the kinetic energy of an impact, since a miniature accelerometer could be easily mounted on the rammer

without adding significant weight. The accelerometer provides information such as the rammer release point, the time of impact and the acceleration during the fall. A numerical integration of the acceleration data produces a velocity profile and more importantly, the impact velocity. A second integration could then be performed over the same time interval and the displacement of the rammer with time determined as well.

From the accelerometer information it was thought that one would be able to compare the theoretical potential energy to the actual potential energy as well as the kinetic energy just prior to impact. This kinetic energy would be a useful check against the energy calculated from the load cell.

However in practice when attempting this configuration, significant issues arose regarding the processing of the accelerometer data due to the vibration of the compactor during operation and the data having a high-frequency noise component in the signal. One of the impact records of a single lift and drop cycle is shown in Figure 3-6.

In the graph in Figure 3-6, it is possible to see the noise in the signal. The acceleration of the rammer was expected to be constant or nearly constant at approximately one g, the gravitational constant (32.2 ft/sec^2). As can be seen, Figure 3.6 shows that no clear acceleration record is evident.

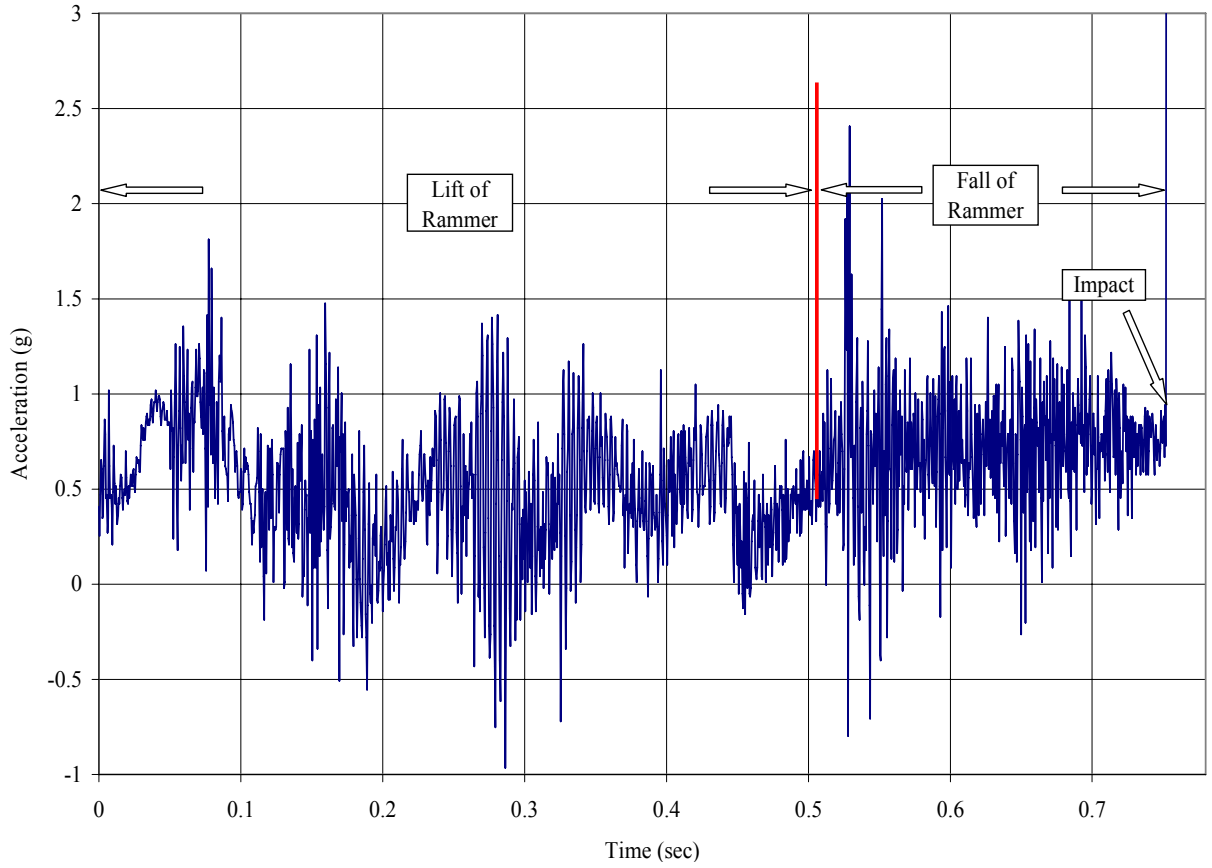

Figure 3-6. Typical acceleration record.

Advanced numerical signal processing utilizing a Fast Fourier Transform procedure was performed on the signal which indicated that during the lift portion of the cycle there was an underlying frequency of 10 Hz. This was attributed to vibration of the motor lifting the rammer. Following the point at which the rammer was released to begin its free fall, the noise frequency increased dramatically. This high frequency is likely caused by the rammer's guide disc contacting the guide rods during the fall. The high noise amplitudes occurred throughout the Fourier transform, making it nearly impossible to remove and obtain an accurate acceleration record. While it is possible that further advanced signal processing algorithms could have been employed, the time and effort required to obtain useful information was considered problematic. Since the goal of this project is to produce a relatively simple and repeatable device that does not

involve advanced data processing and lengthy computational effort, it was decided to abandon this approach and look at yet another alternative concept.

3.3.4 Development of the Photo Gate

Work began on a more direct way of measuring velocity, in order to compute the kinetic energy of the rammer assembly. A search for available velocity sensors was conducted and several transducers were identified. However due to the constraints of the testing environment (i.e., no added mass to the rammer, clearance issues, etc.), nothing was found that would work for this application.

Thus, obtaining an average velocity rather than an instantaneous velocity concept was pursued. Average velocity is readily computed by accurately measuring an elapsed time over a known distance. Equation 3-2 below provides results sufficiently close to the instantaneous velocity at impact as long as the distance over which the time measurements are taken are sufficiently small. This is illustrated mathematically by analyzing the limits of Equation 3-2 as Δd approaches zero, yielding the instantaneous velocity of the rammer. However, physically this is not possible as there is no way to measure change in time as the rammer passes a single point along its path.

$$\text{Velocity} = \frac{\Delta d}{\Delta t} = \frac{d_2 - d_1}{t_2 - t_1} \tag{3-2}$$

In order to apply this method, the rammer instrumentation needed to be set up to begin a trigger timer as the rammer passed a known point just prior to impact and a second sensor to measure the Δ time as the rammer passed a second point slightly closer to the point of impact. The second time measurement is then subtracted from the first and dividing by the distance between sensors, an average velocity is computed. By measuring the distance between the sensors with a set of calipers accurate to $1/1000^{th}$ of an inch, the distance between the sensors

can be accurately measured. These measurements can then be inserted into Equation 3-2 and the velocity just prior to impact evaluated.

While investigating this concept, it was felt that the Hall effect or proximity sensors might be a viable choice. However, further investigation showed that it would be virtually impossible to mount such a assemblage of transmitters/receivers close to the point of impact without creating measurement errors. Thus, it was decided that another type of sensor would be investigated.

3.3.5 The Infrared Photo Gate

Based on the fact that the data acquisition system can readily read voltages, the idea emerged that a photo gate or optical switch might work. It is based on the principle that when a phototransistor detector senses an emitter diode's IR light, a voltage is produced. In addition, when the phototransistor detector does not sense the emission, the voltage remains zero. Three of these emitter/detector pairs were then planned to be mounted in sequence and used to obtain the change in time. The rationale for using three sensor pairs rather than two was based on the fact that if time measurements were known at three locations, then three separate velocity calculations were possible. These additional velocity measurements could then be used to determine if the velocity of the rammer was within an acceptable profile.

Several infrared emitter and detector pairs were purchased with the appropriate resistors in order to create the switch configurations. Switch operation was then monitored with a voltmeter for preliminary tests and found to perform properly. They were then mounted to a compaction mold base plate so that an emitter and its corresponding detector were on opposite sides of the plate (Figure 3-7).

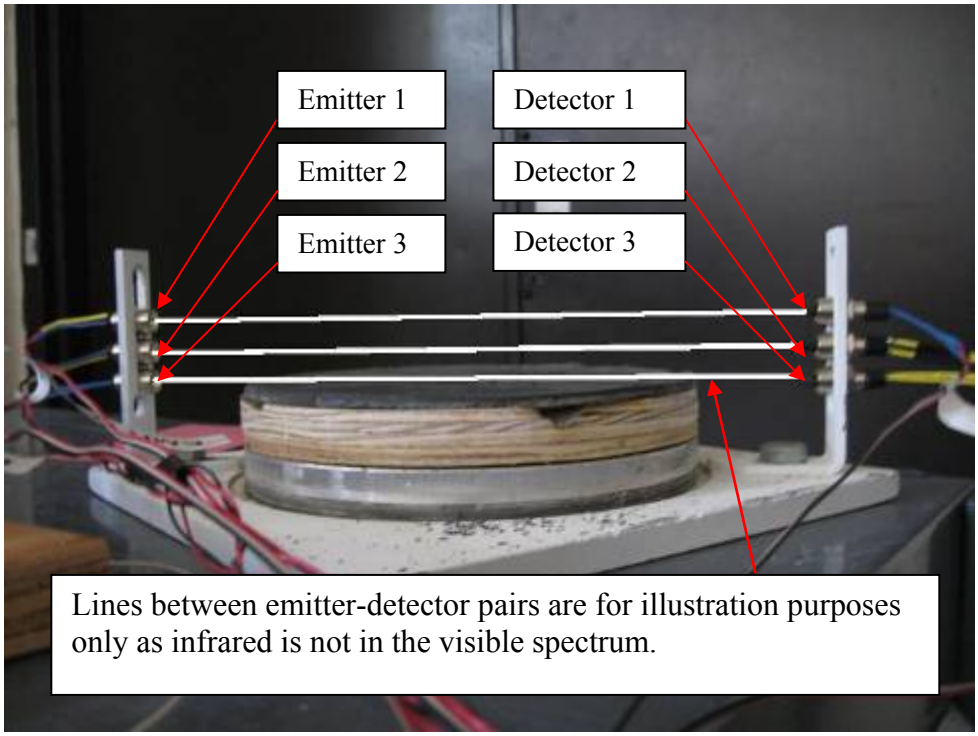

Figure 3-7. Standard test setup for infrared photo gate.

In order to prevent rammer bounce, an impact pad was added to dampen the blow. Various materials were tested, since it is important for it to not undergo any permanent deformation. This is because the distance from the surface to the last detector would then change slightly and alter the velocity calculations. Having a proper impact pad also allowed for the lower emitter and detector pair to be aligned such that the voltage drop will occur the instant the rammer comes into contact with the pad.

After numerous tests, several issues became evident. First, there were occasional voltage spikes prior to switch detection as well as random voltage irregularities. Effort was spent trying to eliminate interference from outside infrared sources, as these were suspected of causing the problem. The increase in voltage prior to impact was determined to come from the reflection of infrared light reflecting off the bottom of the rammer's face prior to the rammer actually breaking the line of sight of the detector. These issues made it impossible to accurately

determine the time of travel. An example of the data obtained from the infrared photo gate is presented in Figure 3-8.

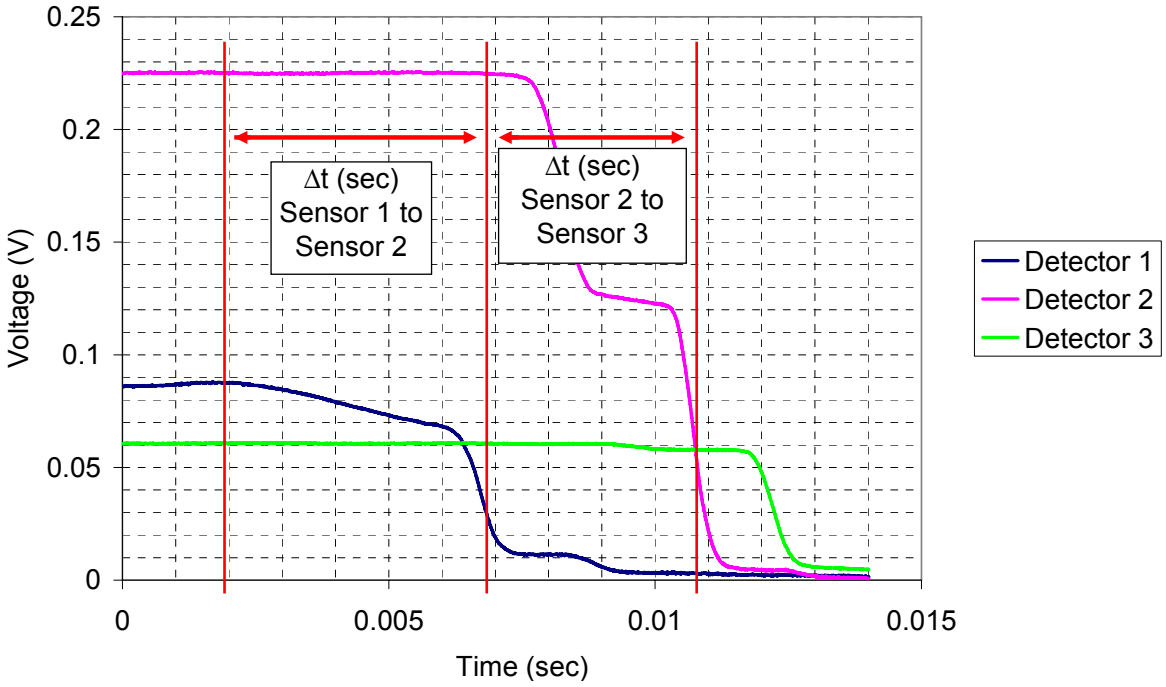

Figure 3-8. Voltage measured from infrared photo detector pairs 1, 2 and 3.

Several rotations of the hammer with ten impacts each were performed and velocities were calculated. These measured velocities were then compared to impact velocities obtained from differentiation of the laser's displacement record. The results are presented in Table 3-2.

Table 3-2 shows the importance in accurate time determination, since small differences in the measured time have a large adverse effect on the velocity calculations. It was determined that for accurate kinetic energy measurement, the infrared emitter detector sensors were not adequate unless significantly improved. Attempts were made to obtain better quality voltage records by replacing the infrared emitted diodes with laser diodes, however, this also proved unsuccessful. Attention was then directed to an existing type of through-beam photo electric sensor which was available on the market.

Table 3-2. Measured Travel Times from Sensors and Corresponding Energy Calculations

Impact	Sensor 1 to Sensor 2 Δt (sec)	Sensor 2 to Sensor 3 Δt (sec)	V_1 Avg Velocity Sensor 1 to Sensor 2 (in/sec)	V_2 Avg Velocity Sensor 2 to Sensor 3 (in/sec)	Kinetic Energy	
					E_1 (from V_1) (ft-lb)	E_2 (from V1) (ft-lb)
1	0.00486	0.00468	87.45	90.81	8.25	8.90
2	0.00314	0.00439	135.35	96.81	19.77	10.11
3	0.00856	0.00435	49.65	97.70	2.66	10.30
4	0.00761	0.00554	55.85	76.71	3.37	6.35
5	0.00680	0.00569	62.50	74.69	4.22	6.02
6	0.00412	0.00417	103.16	101.92	11.48	11.21
7	0.00462	0.00411	91.99	103.41	9.13	11.54
8	0.00656	0.00748	64.79	56.82	4.53	3.48
9	0.00670	0.00442	63.43	96.15	4.34	9.98
10	0.00254	0.00542	167.32	78.41	30.21	6.64

3.3.6 Development of a Photo Electric Gate

Traditionally, photo electric sensors have been utilized in manufacturing for product detection, but it was hypothesized and later proven that these sensors were able to effectively detect the presence of the rammer as it passed by a sensor in the same manner that the infrared sensors operated. The primary issue with these devices was their switching response times since all of the available models were digital (compared to analog).

After significant searching, Keyence Corporation had the precise instrument to resolve the issues encountered in the testing of the infrared photo gate. After reviewing the specifications, two Keyence FS-M1H fiber optic amplifiers were purchased. These sensors operate on the same principle as the infrared photo gates in detecting the rammer's presence. However, they boast more advanced electronic features for velocity measurements.

The Keyence M1H fiber optic sensors operate digitally. They are essentially a switch in the traditional sense of the word, with the output from the sensor either a fixed portion of the excita-

tion voltage or zero. This function allows for simple determination of when the rammer passes the line of sight of the detector. While detection remained an issue for the infrared sensor, it was not the only issue solved by using this instrument. The fiber optic sensors also offer a fixed sampling period of 20 microseconds which by calculation is more than sufficient for a spacing of 0.950 inches, the anticipated sensor spacing. These features alone are reason enough to utilize these sensors. In addition, they feature pair specific light modulation to prevent cross talking and false detections of the rammer which ensure accurate reporting of rammer detection times.

The sensor heads were mounted in the same configuration as the infrared sensors on the base plate of the compaction mold as a pair for testing (Figure 3-9).

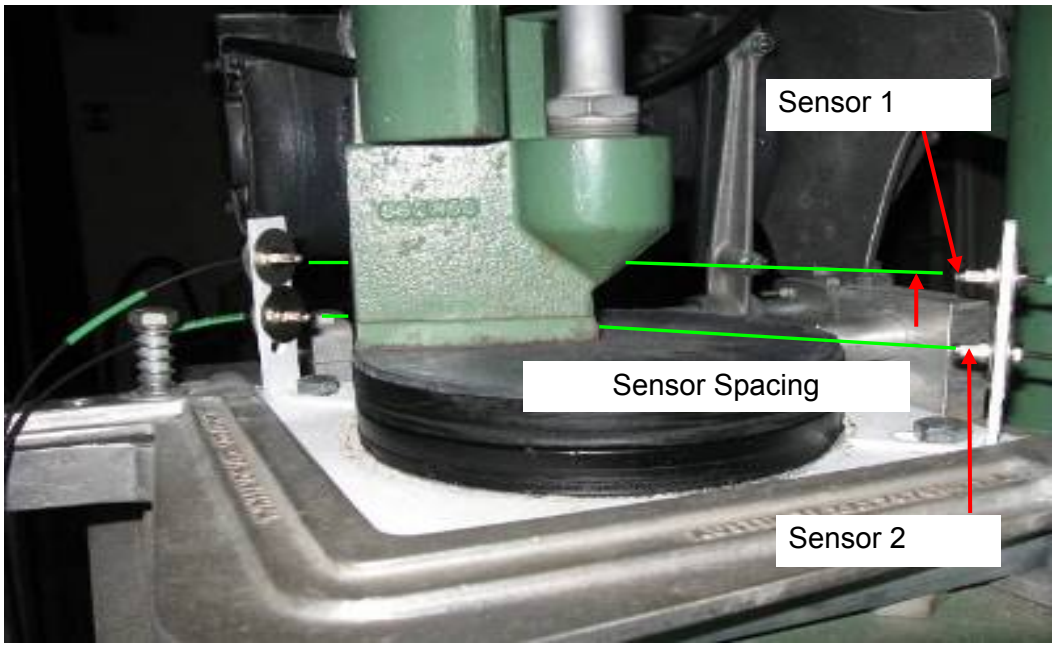

Figure 3-9. Base-mounted setup for fiber optic photo gate.

3.4 Development of the Load Cell System

During the development stage of measuring the impact kinetic energy, several compaction units were observed in various laboratories. It became apparent during these laboratory visits that while all of the machines were calibrated per AASHTO standards, there was one major

difference that appeared fairly regularly. As per soil compaction standards, the compaction machine must be mounted on a rigid concrete base with a mass greater than 200 lb (AASHTO T-99 and T-180 Note 7). All the machines observed did satisfy this requirement, however, some had a plywood cushion beneath their steel base plates while others used aluminum spacers. In fact, several had nothing supporting their bases.

As previously shown in Figure 2-3, an observable shift in the maximum dry density and the optimum moisture content occurs that is not consistent with AASHTO specifications. This is likely due to the varying amount of energy that is transferred into the soil during compaction. With the understanding of dampening and its energy effects, the possibility that the base stiffness itself may have a significant effect on soil compaction was surmised. In order to quantify what effect the base stiffness has on energy transfer, standard compaction mold base plates, 4 and 6 inch respectively, were instrumented with both a PCB 200C20 load cell and a PCB M352A60 accelerometer. A 0.25-inch thick piece of neoprene pad was then cut to fit the impact surface of the load cell to protect it during impact. These base plates were then fastened to the base of the machine and clamped in place. The compactor's rammer could then be set up at the standard drop height angled slightly from the impact pad to account for the rotation of the rammer. The machine could then be switched on for a single impact on the face of the load cell.

Due to the accuracy and ease of repeatability of this test, it could then be used to measure the base stiffness of a sample population of compaction machines. From this information, the energy losses due to variables in the mounting configuration of the machines could be quantified.

CHAPTER 4
VALIDATION OF THE PORTABLE CALIBRATOR

4.1 Validation of the Photo Electric Gate

In order to ensure accurate velocity measurements using the fiber optic photo gate, it was critical to compare the velocities measure with a known velocity. Thus, the laser displacement sensor was again mounted above the mechanical compaction machine and used to continuously measure the displacement of the rammer. The photo gates were mounted in the configuration pictured in Figure 3-9 as shown in Section 3.3.6. The mechanical compaction machine in the T-180 configuration, was then switched on and allowed to complete five full rotations of the impact rammer, in this case several of the impacts were missed by the photo gate when the rammer was near perpendicular to the sensor as discussed previously. For the 50 impacts, 29 were captured by the photo gate. However, this is not a problem, since the operator would simply wait until a sufficient number of data points are collected.

The displacement record from the laser was then parsed such that the data for the fall could be analyzed. This data was then processed in a very similar way to that presented in Figure 3-4. However, through a study of the laser displacement data, the acceleration was not constant. Using a central difference scheme on the displacement versus time records, accelerations for points along the time record were calculated directly. These results are presented in Figure 4-1.

The results clearly show the acceleration changes with respect to time linearly throughout the fall event of the rammer. This prevents use of a second-order equation for derivation of impact velocity of the rammer as a valid method. Rather, it dictates the use of a third-order polynomial equation for the description of the rammers fall with displacement in order to allow the linear change in acceleration with time.

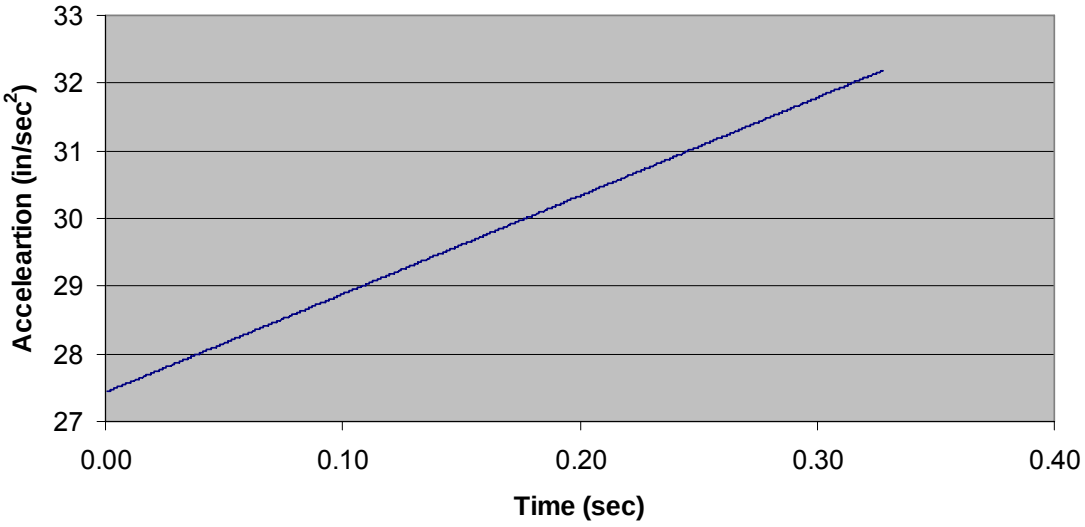

Figure 4-1. Linear acceleration of rammer during T-180 fall.

Thus, a third-order equation was used to determine the impact velocity of the rammer at the time of impact. Impact velocities were thus calculated from the laser displacement data and compared to the impact velocities measured using the photo gate mounted on the compaction mold base plate. The results of this T-180 test configuration showed a mean impact of 14.19 ft-lb with standard deviation of 0.24 as measured by the displacement laser. The photo gate mean kinetic energy was 14.30 ft-lb with a standard deviation of 0.99. The results from this test show fairly poor agreement between the two measurements. These discrepancies are due to the distance between the emitter and detector optical fibers as well as the difficulty in precisely aligning the sensors. Since the mold and appurtenances limit the installation height to 6 inches, and to bypass the issue with the rammer being perpendicular to the photo gate and its signal being missed, the sensors were then relocated to the top of the compactor. Now, the time that the rammer breaks the line of sight of the detector and the time that the line of sight is restored is used. The only line of sight of each other, for both sensors, is when the rammer is in contact with the impact pad (Figure 4-2).

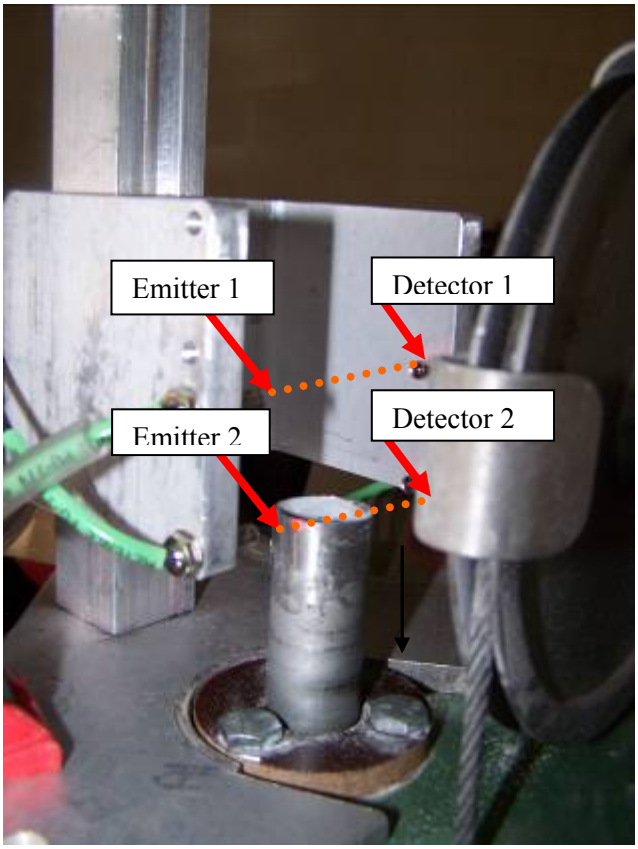

Figure 4-2. Sensor alignment on compaction machine.

This setup was verified to operate correctly 100% of the time regardless of the orientation of the rammer. The verification study was performed again using the laser displacement record and the velocity of impact measured by the photo gate. The test operated for five complete rotations, and all 48 impacts were recorded by both sensors. A third-order polynomial derivative to describe the impact velocity of the rammer was compared to the velocity measured with the photo electric gate. This testing configuration resulted in much better agreement than the base mounted configuration. These results have been summarized in terms of the rotation of the hammer as well as in terms of the entire population of rotations. However, for the summary of all rotations, it is important to note that the first rotation has been removed from the data set due to the improper function of the photo gate during this initial test run (Table 4-1).

Table 4-1. Summary Statistics for Validation Study Hammer Rotations

		Velocity Measured Using Photo Electric (in/sec)	V_{imp} Laser (in/sec)	Kinetic Energy Measured (ft*lb)	Kinetic Energy Calculated (ft*lb)	Potential Energy Measured (ft*lb)	Percent Difference between Kinetic Measured and Calculated (%)	Percent Difference Between Kinetic Measured and Potential Measured (%)
Rotation 1	Average	114.24	115.84	14.09	14.48	15.27	2.73	7.77
	Standard Deviation	0.70	0.81	0.17	0.20	0.07	0.55	0.97
Rotation 2	Average	115.85	115.76	14.48	14.46	15.28	-0.16	5.19
	Standard Deviation	0.66	0.60	0.17	0.15	0.04	0.68	1.12
Rotation 3	Average	115.73	115.65	14.46	14.43	15.29	-0.15	5.44
	Standard Deviation	0.63	0.63	0.16	0.16	0.04	0.63	0.90
Rotation 4	Average	115.82	115.61	14.48	14.42	15.30	-0.37	5.35
	Standard Deviation	0.79	0.87	0.20	0.22	0.03	0.67	1.32
Rotation 5	Average	115.91	115.95	14.50	14.51	15.30	0.07	5.27
	Standard Deviation	0.86	0.78	0.22	0.20	0.06	0.73	1.26
All Impacts in Rotation 2-5	Average	115.83	115.74	14.48	14.46	15.29	-0.15	5.31
	Standard Deviation	0.72	0.72	0.18	0.18	0.04	0.67	1.12

This table illustrates the precision in the measurement of mean velocity for each rotation of the rammer. With the removal of the data acquired from the first rotation of the rammer, the summary statistics of the population are based on 39 impacts. The mean impact velocity measured using the photo electric gate was within 0.21 in./sec of the actual impact velocity of the rammer as measured by the displacement laser. This is less than a 0.2% difference. This maximum difference in measured velocities thus resulted in a maximum percent difference in the mean energy calculations of 0.37 ft-lb while the other three useable rotations resulted in an absolute percent difference of less than 0.16 ft-lb.

As an additional step to verify the accurate measurement of the impact energy, attention focused on the standard deviation of the rammer's impact energy for each rotation. Analysis shows there to be good agreement between the standard deviation of the energy of each individual rotation as well as for the population as a whole for each rotation of the hammer.

From this study it was verified that the velocity measured using the photo electrics mounted on the top of the compaction machine at a spacing of 0.950 inches is sufficiently accurate to establish the velocity at impact of the compaction rammer, as well as the variance of the energy during operation.

4.2 Accuracy of the Instrument

In an effort to verify that the Keyence M1H photo electric sensors accurately measure the velocity of a passing object, a time study was performed that utilized the operational frequency of the sensors and the distance between them. The design distance of the sensors was set at 0.950 inches. For an AASHTO T-180 compaction test, Newtonian physics shows that for a free fall of exactly 18 inches, an impact velocity of 117.89 inches per second should result. This velocity was then used to determine the time required for the rammer to travel a distance of 0.950 inches or approximately 0.00806 seconds.

The operational frequency of the M1H photo electric sensors is 50 kHz (50,000 samples per second). This means that every $1/50{,}000^{th}$ of a second, the sensor outputs a voltage corresponding to its line of sight. This results in an accuracy of 0.00002 seconds in the detection of the rammer at either sensor. Thus, for a two-sensor system, the precision in the time of travel measurement could be off by a maximum of 0.00004 seconds.

In order to determine the effect a time of travel error of 0.00004 seconds might have, this tolerance was applied to the 0.00806 time determined previously. A maximum error was found to result in an impact velocity range of 117.28 to 118.45 inches per second. This translates into a range in energies from 14.84 to 15.14 ft-lb, resulting in a tolerance of ±1% of the actual energy for a single impact.

It should be noted that this is the maximum error for any given impact. This error in time determination is considered random error and could thus occur for either sensor, translating into ± 0.00002 seconds and the mean centered about 0 seconds. As such, as long as multiple impacts are being measured, any error is offset when taking the average of the values.

4.3 Validation of the Testing Procedure

4.3.1 Photo Electrics

The next step in the validation of the photo electric sensor was to validate the testing procedure. The same data that was used in the sensor validation study was used. However, now that it has been verified that the photo electric velocity measured was valid for use as the impact velocity, only these values were utilized. A bootstrap analysis was performed for each hammer rotation in an effort to verify that the mean energy for a single rotation of the hammer was representative of the mean of the multiple rotations of the machine. In addition, the variance of a single rotation of the rammer was representative of the variance of the machine.

For this analysis, the mean energy for each rotation was found to be the mean of the bootstrap for all cases. In comparison to the mean, the variance of the bootstrap was found to be small and in all cases less than 0.0024. Since this value was small and the mean of the sample was equal to the mean of the bootstrap, statistically, the mean for any single rotation is representative of the mean of the machine.

In an effort to validate the variance of the mean energy for a single hammer rotation, the bootstraps for each rotation were again utilized. The bootstrap mean variance for a single rotation was compared to the variance of the energy for each rotation and found to be within ± 0.01 of the variance of the rotation.

Another method used to determine if a single rotation is enough to quantify the variance of the machine is to take the coefficient of variation of the bootstrap standard deviation. This is done by Bootstrapping the kinetic energy measurements of a single rotation 4000 times. The standard deviation of the boot strap standard deviation is then calculated and divided by the mean of the bootstrap standard deviation. A small value of the COV of the bootstrap standard deviations indicates that there are enough samples to accurately quantify the variance of the machines kinetic energy. If this value is small, that indicates the variance of the kinetic energy is representative of the machine.

4.3.2 Compliance Instrumentation

In an effort to ensure the repeatability of the results of the load cell and accelerometer base compliance device, several tests were run at UF and FDOT's SMO. These tests consisted of placing the compaction mold base plate in the compactor, using the standard base plate vise. Several impacts were then created on the face of the load cell and recorded.

The data generated by the impacts were then plotted as load and acceleration with respect to time. The results of these tests showed the ease of accurate repeatability for a given machine (Figures 4-3 and 4-4). This is due primarily to the accuracy under which these instruments have been calibrated.

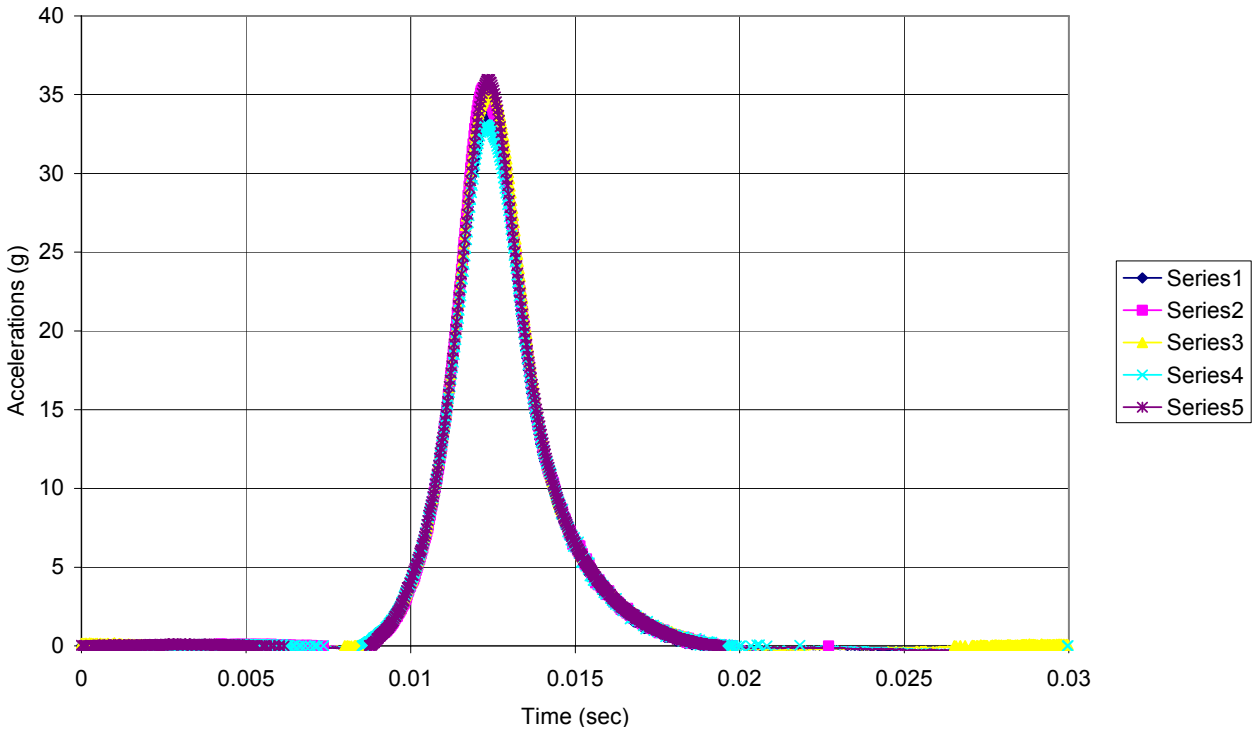

Figure 4-3. Typical acceleration and time duration plot for base compliance measurement.

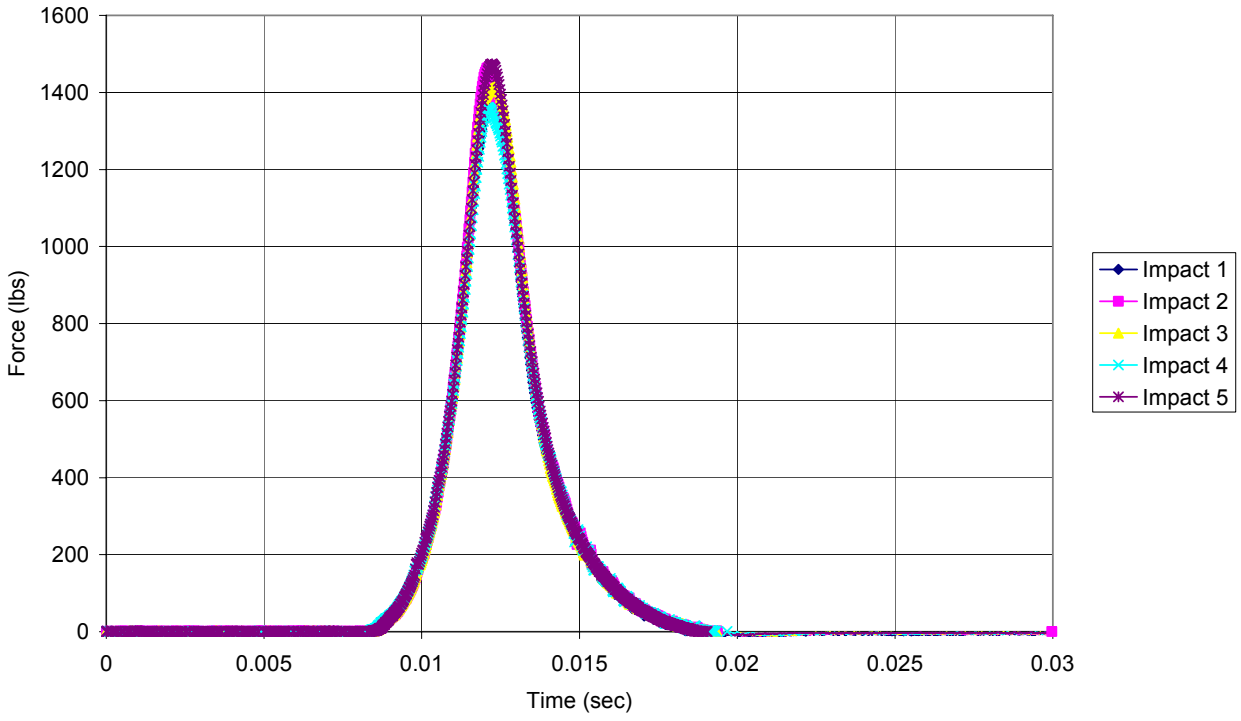

Figure 4-4. Typical force and time duration plot for base compliance measurement.

CHAPTER 5
LABORATORY TESTING AND ANALYSIS

5.1 PDEC Setup Description

Use of the portable dynamic energy calibrator (PDEC) relies on two main components, the photo electric gate and a base system compliance mold. The photo electric gate pictured in Figures 5-1 easily mounts on the top of the compactor using two C-clamps. Adjustment to the photo electric gate then needs to be performed to ensure that the velocity is measured across the last 0.950 inches of travel or just prior to the rammer's impact on the impact pad. This can be done by loosening the adjustment thumb bolts on the back of the mounting post and sliding the "C" channel section vertically until sensor pair 2 is at its switching point (see Figure 5-2 as well as Figure 4-2 in Section 4.1 and Appendix A).

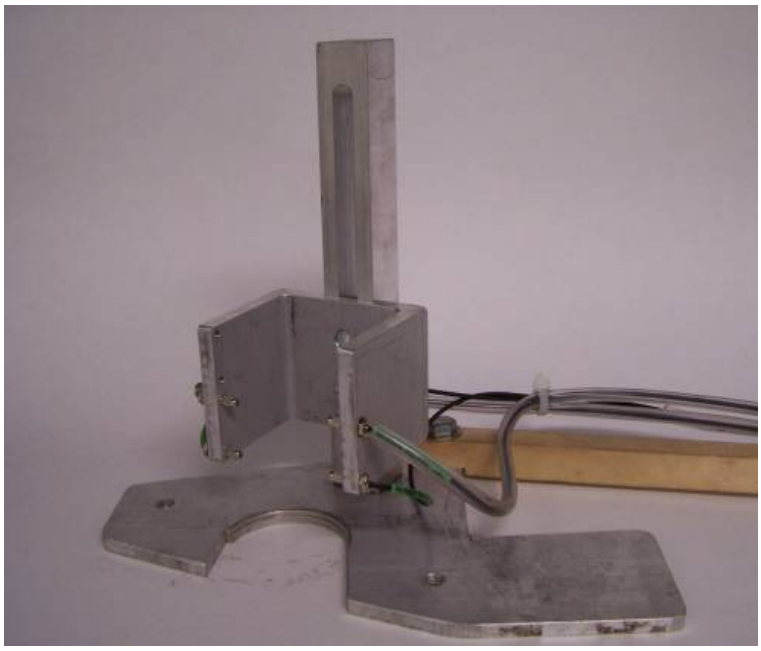

A

Figure 5-1. Photo electric gate. A) Front view. B) Rear view.

B

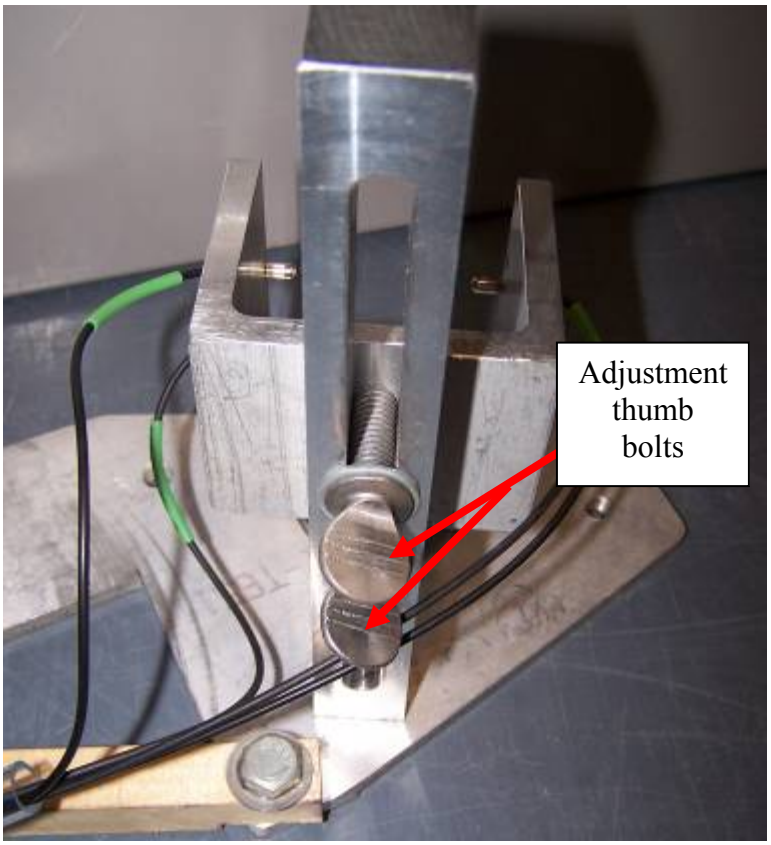

Figure 5-1. Continued

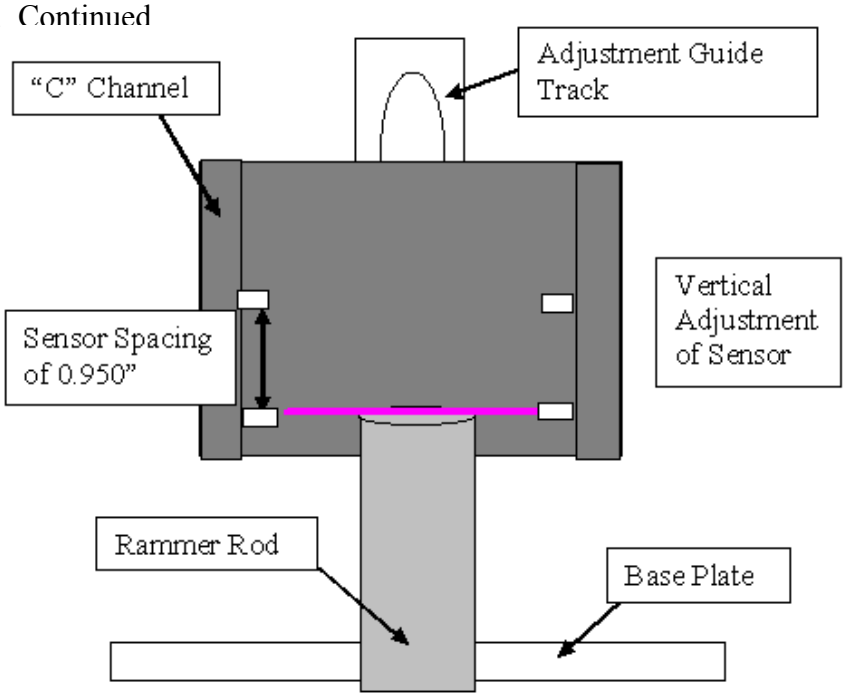

Figure 5-2. Illustration of rammer rod at switching point of sensor 2.

With the plywood and sorbothane impact pad in place, the compaction machine can be started. The digital output from the Keyence M1H photo electric sensors are simultaneously sampled by a Measurement Computing 1608H data acquisition system at a rate of 50,000 samples per second (50 kS/s) and the laptop converts it to the impact velocity of the rammer (Figure 5-3). Since the rammer mass (including the rod) was determined at the time of testing, by measuring the impact velocity, the kinetic energy of the rammer for each impact was calculated.

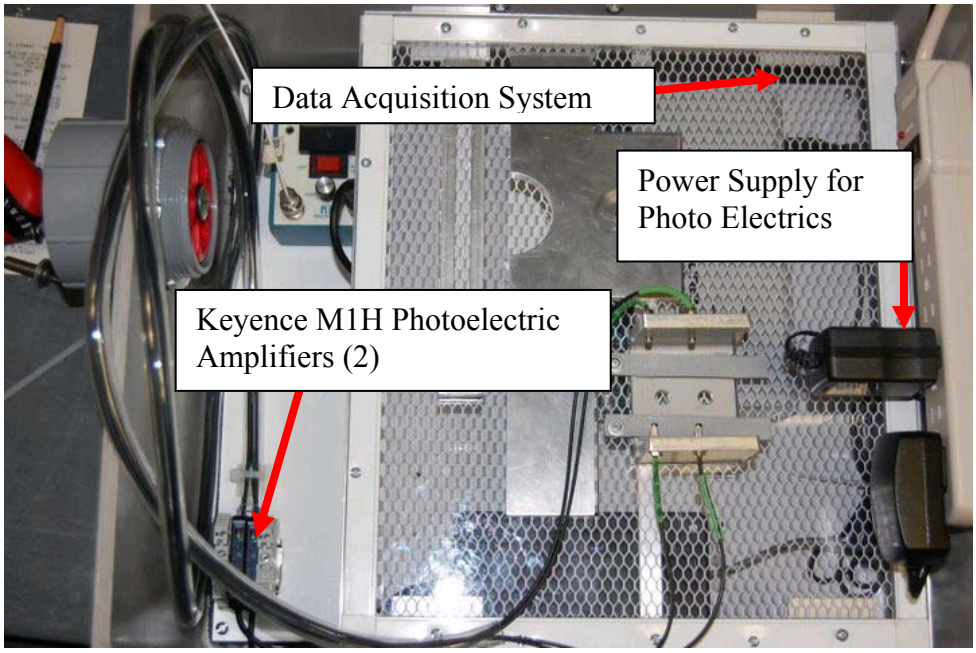

Figure 5-3. Data acquisition system setup and sensors.

Following the velocity measurements, forces and accelerations from a single rammer impact are measured at the base of the compactor (Figure 5-4). The device is stationary and there is a single impact location, so the rammer must be positioned correctly to impact the force sensor. Figure 5-5 shows an instrumented 4-inch mold assembly with a force impact sensor and 500-g accelerometer affixed to the base. The respective mold assembly, 4-inch or 6-inch (not shown), is placed into the compactor and used to measure single impact forces and accelerations.

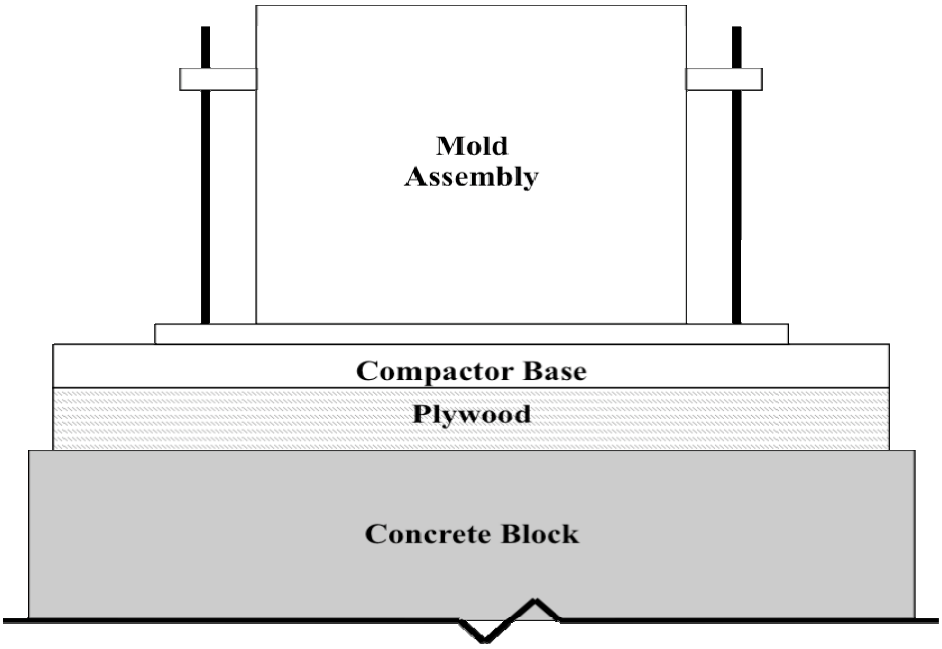

Figure 5-4. Base system configuration with mold assembly.

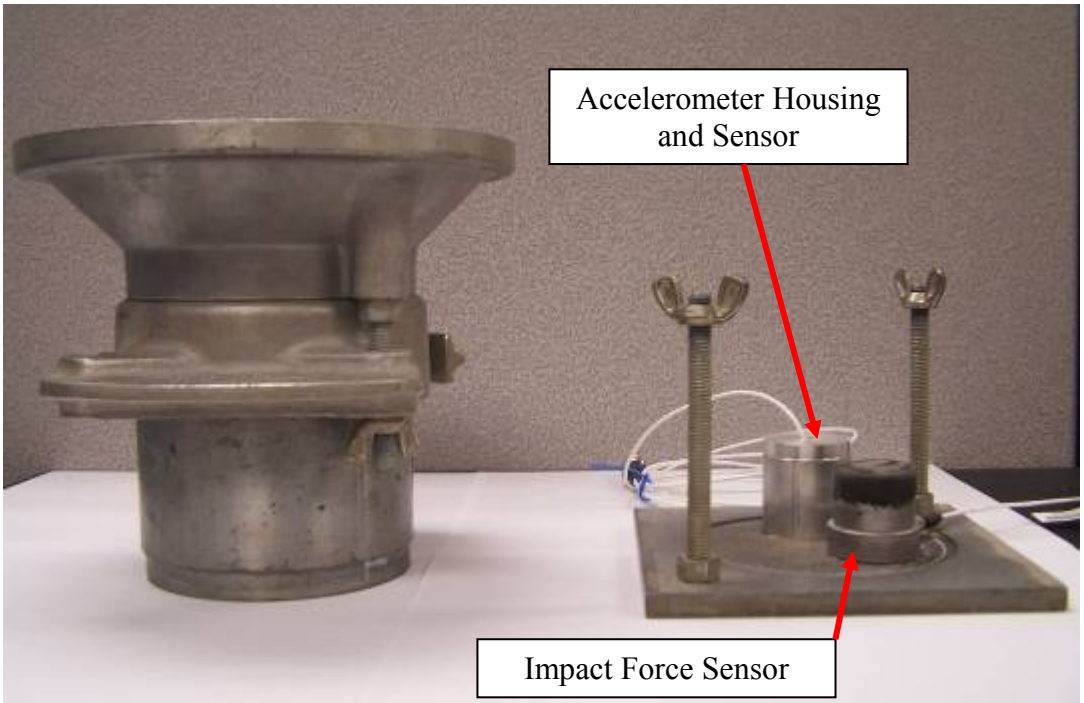

Figure 5-5. Instrumented mold assembly.

The force sensor is positioned such that contact is made with it at the centroid of the rammer. The accelerometer is located two inches away from the force center, center-to-center. The sensor instruments are connected to the portable data acquisition system/notebook PC for data sampling (40,000 samples per second (40 kHz)) and storage.

5.2 Testing Program Overview Using PDEC Instumentation

The PDEC was taken to 16 state and independent compaction laboratories in Florida for testing on T-99 and T-180 mechanical compactors. Laboratories were identified per FDOT districts as ones certified to perform T-99 and T-180 tests. Districts 2, 5, and 7 (see Figure 5-6) were visited.

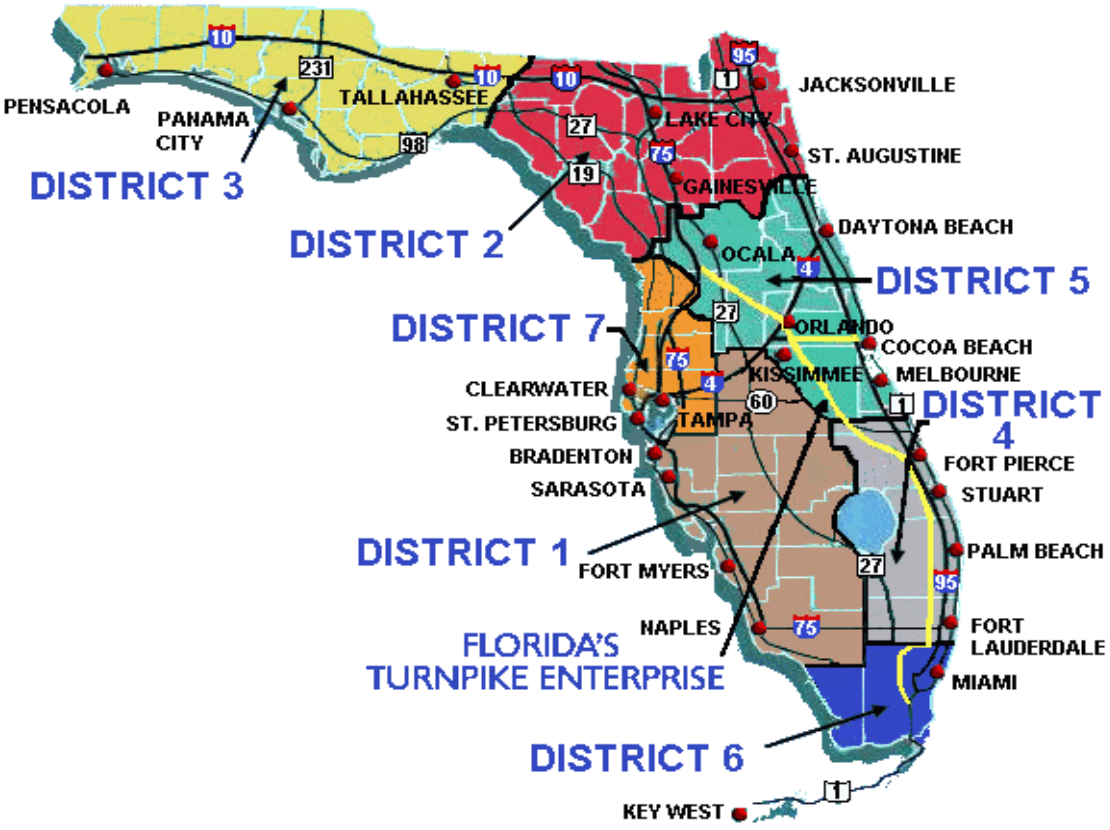

Figure 5-6. FDOT district map

The data obtained provided a sample population with summary statistics, such as the mean, median, and standard deviation in impact velocity (function of drop height), kinetic energy

(function of mass and impact velocity squared), and compliant characters (peak force, peak acceleration, peak time). The Modified (T-180) Proctor configuration was most frequently encountered in the laboratories. Thirty T-180 compactors and four T-99 machines were tested. The compactors were set on a foundation of cast-in-place concrete or block with aluminum, steel or plywood cushions between the machine base and the foundation (Figures 5-7). The results and analysis presented are from the thirty T-180 compactors.

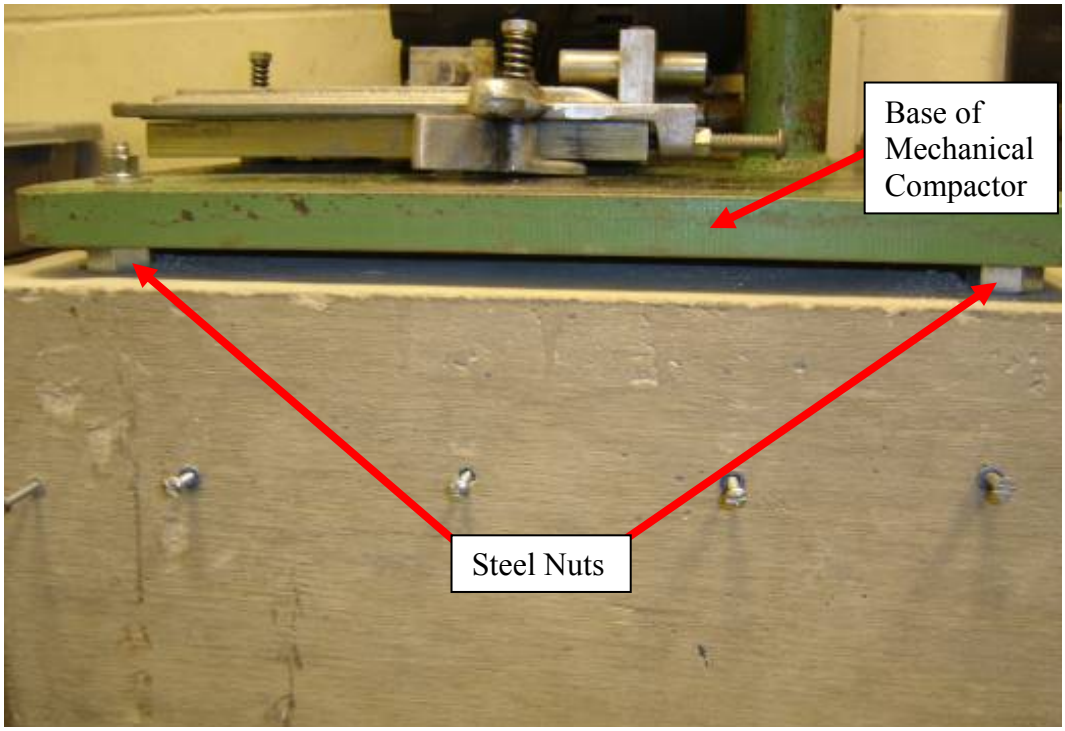

A

Figure 5-7. Compactor foundation. A) Steel cushion. B) Plywood cushion.

B

Figure 5-7. Continued

5.3 Testing Results and Analysis of PDEC Data

5.3.1 Kinetic Energy Assessment

Impact velocity was measured for each machine. The kinetic energy of each impact is calculated from the impact velocity and rammer mass of each machine as shown in Equation 1-2. The kinetic energy data was summarized for the variance per machine and variance among all the machines by considering the mean per machine. Figure 5-8 presents the frequency distribution of the mean energy of the sample population. The mean energy is taken as the sum of all kinetic energies in a single round of rammer impacts (8-10 impacts) divided by the number of impacts and represents a single machine.

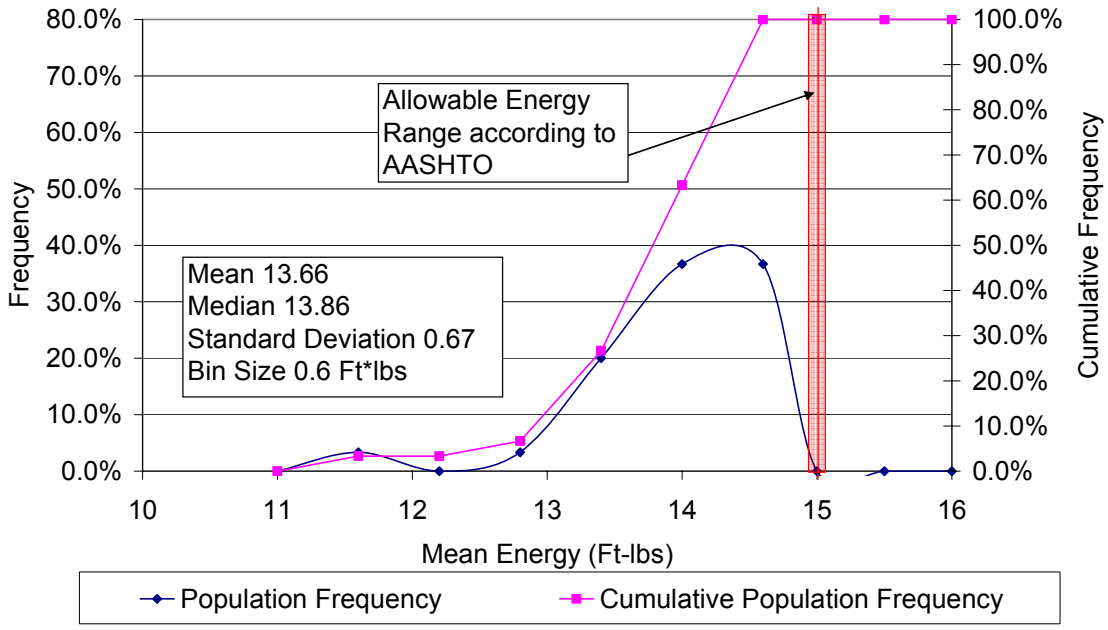

Figure 5-8. Frequency distribution of mean energy data.

A bootstrapping procedure was then performed to ensure that the sample was representative of the entire population of machines. The functionality of bootstrapping is a numerical simulation by re-sampling real data. The process of bootstrapping takes the values of the sample population and randomly selects a value a specified number of times to generate a single bootstrap. From those values randomly selected, summary statistics can be used to describe the characteristics of that bootstrap, namely the mean and variance. In an effort to ensure enough repetition in the bootstrap procedure, 4,000 bootstraps were generated. The mean of all 4,000 was then calculated as well as the variance and mean of the bootstrap variances. These summary statistics for the bootstraps are then used to make statistical inferences for the entire population. In order to verify that the sample is sufficient to represent the population, two key values are analyzed: the variance of the bootstrap variances; and the mean variance of the bootstrap. As long as the variance of the bootstrap variances is small, it indicates that enough samples were

taken from the population to establish the variance of the bootstrap population accurately. In this case, the mean variance of the bootstraps can then be compared to the variance of the sample population. Good agreement of these values indicates the sample is representative of the population.

From the sample of thirty machines, a bootstrap analysis was performed on thirty values (with the possibility of repetition) randomly chosen to generate each bootstrap. From the summary statistics, the mean of the variance for all of the bootstraps is 0.43. When compared with the variance of the sample population (which had a variance of 0.45 (0.67^2)), it is apparent they are in excellent agreement. This shows that the population sample of thirty machines is representative of the entire population of proctor compaction machines. Next, the variance of the bootstrapped variances was calculated to be 0.03. Since it is significantly smaller than the mean variance of the bootstraps, it shows there is high accuracy in the determination of the variance of the population using those thirty machines.

Also using the bootstrap method, one is able to gain more confidence in the distribution of the data collected. The bootstrap procedure quantifies the uncertainty of the mean through statistical inference. Shown in Figure 5-9 is the frequency distribution of the bootstrap procedure for the 30 mean energy data values. The distribution type suggested by Figure 5-9 is normal with a mean and median very close to that of the sample population (13.66 ft-lb and 13.86 ft-lb, respectively). The distribution of the variance of the data mean is small ($0.3^2 = 0.09$). A comparison of the data and bootstrap distributions show good agreement. It is important when comparing the bootstrap distribution and the data distribution for one to note the summary statistics, to see if the mean energies coincide and the median values are close to one another.

For example, the median value for the bootstrap is within 1.5% of the median value for the laboratory data set.

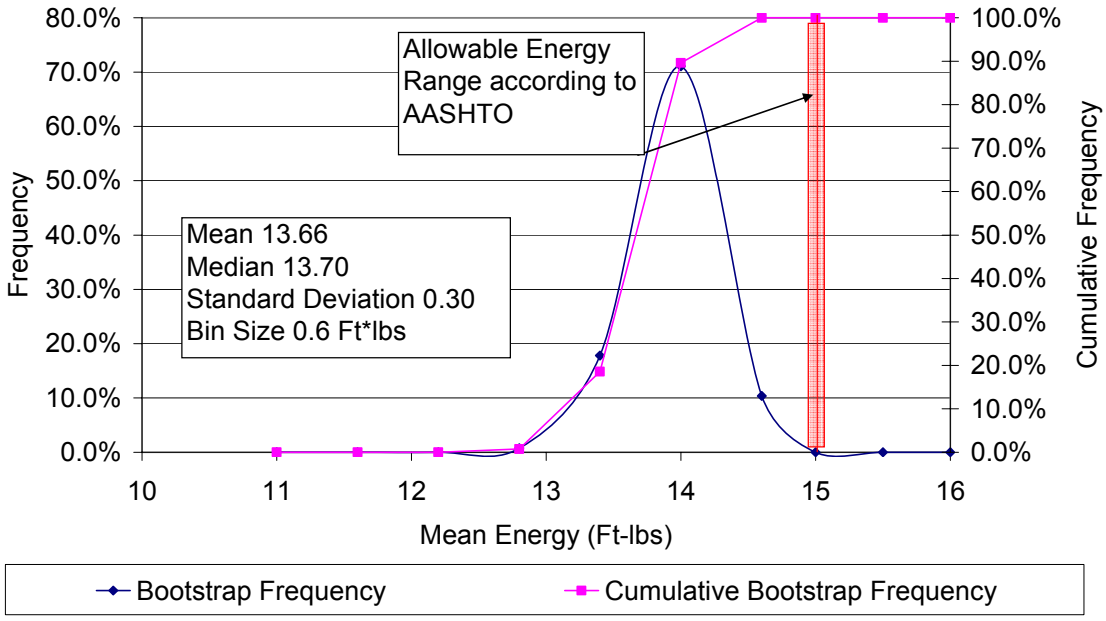

Figure 5-9. Bootstrap frequency distribution of mean energy.

Figure 5-10 shows the frequency distribution of all the calculated kinetic energies from the data; these are not a representation of the mean values. These are all energies for a single round of impacts on each machine. Compared to Figure 5-8, Figure 5-10 provides better insight into the percent of the population below the allowable range of energy based on AASHTO standards of rammer mass and drop height. Through close examination and interpretation of Figure 5-10, it is possible to see that the cumulative frequency portion of the plot showed no impacts above the AASHTO specified energy. Rammer masses were measured for each machine and it was observed that all rammer masses were within the specified tolerances. This indicates that low energy available for compaction stems from low impact velocities.

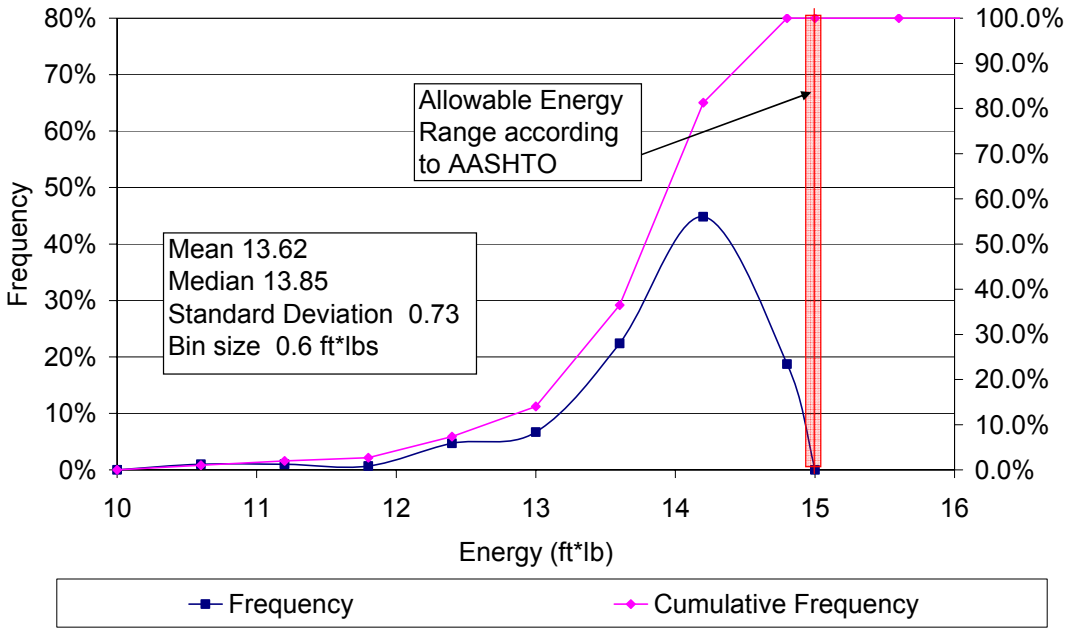

Figure 5-10. Frequency distribution of all energy data.

With the summary statistics and the mean velocity and energy, Figures 5-11 and 5-12 were generated as scatter plots. In this case, a scatter plot provides a good visual identification of machines which may be outliers of the population and where to look for the sources of error. For example, in Figure 5-11, there is an extreme outlier with a standard deviation of approximately 4.5 and mean velocity of 103 inches/second. Since the velocity, V, is a function of the drop height and free fall acceleration, this indicates there is a problem with the machine not consistently dropping the mass from the same height and/or large inconsistent frictional impedance during the free fall acceleration. A point near the low end of the standard deviation, for example 0.5, indicates a consistent deviation about the mean for this machine, essentially showing that the drop height and or the frictional forces on the rod are consistent for each fall of the rammer. According to drop heights in AASHTO and ASTM standards, the range of allowable velocities based on free fall is shown in red in Figure 5-11.

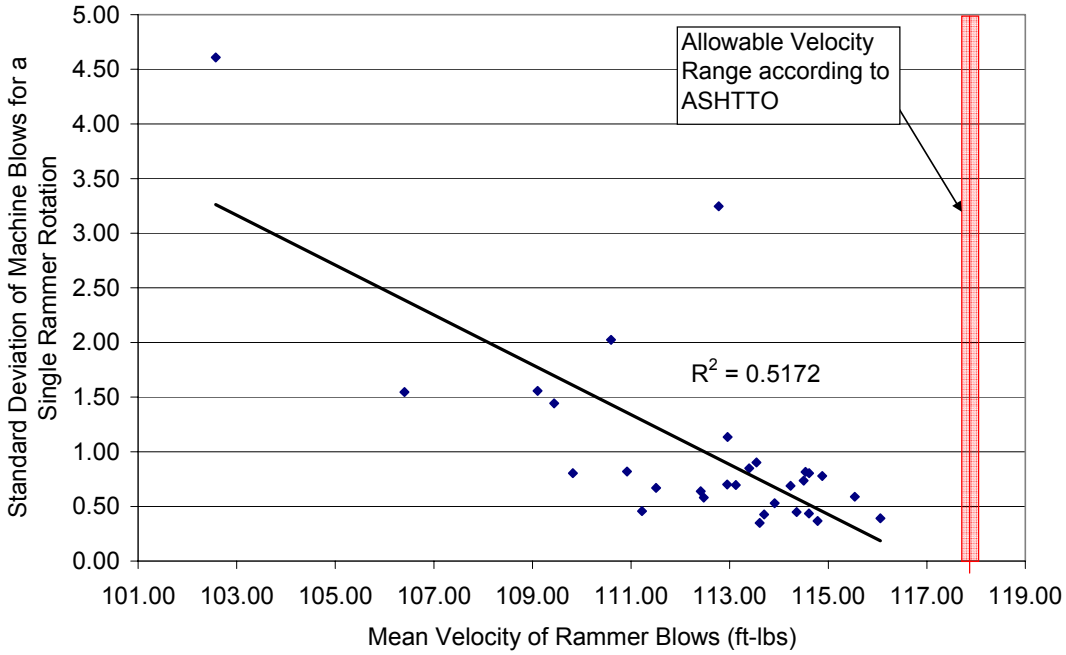

Figure 5-11. Scatter plot of energy standard deviation versus mean velocity.

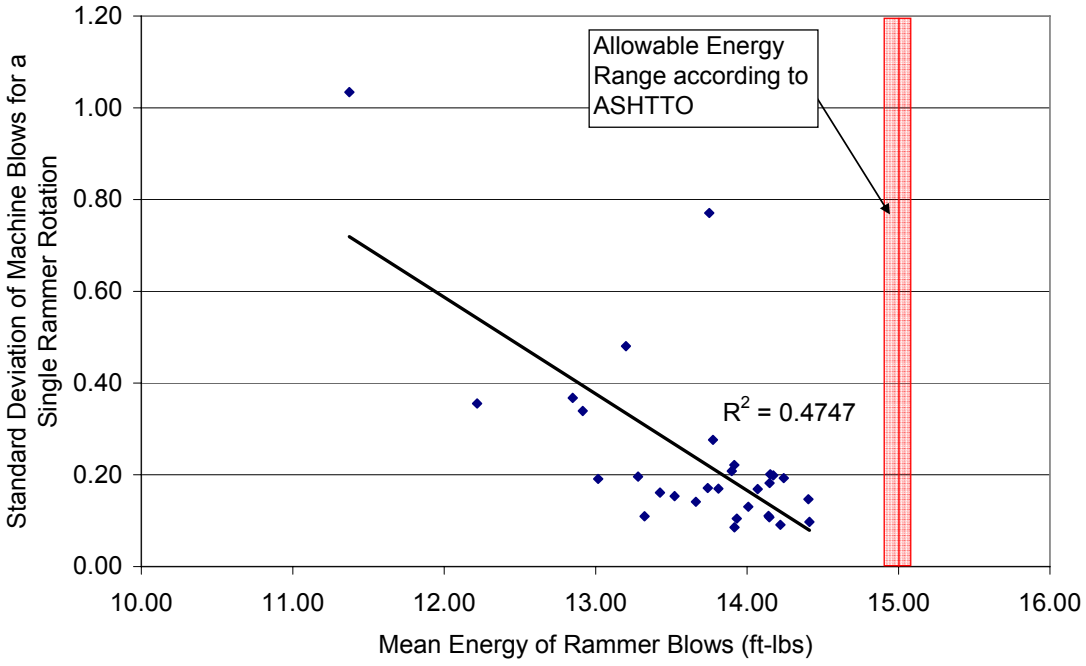

Figure 5-12. Scatter plot of energy standard deviation versus mean energy.

Figure 5-12 shows the scatter plot for the mean kinetic energy of the sample population. The results show a definitive trend in the data. That is to say, machines that display a low standard deviation in the energy delivered by each blow are more likely to have a higher mean energy, whereas machines that have a large energy standard deviation typically have a lower mean energy associated with the machine. In general, the majority of the population has small standard deviations (≈ 0.10 to 0.20) and all are below the range of allowable energy according the AASHTO standards T-180.

5.3.2 Manual Compaction Rammer

In order to establish a baseline for understanding the kinetic energy measurements from the mechanical compaction machine, testing was performed to quantify the typical kinetic energy available from a T-180 manual rammer.

Six manual T-180 compaction rammers were tested. Three of the six were different commercial models. The rammers were attached to a temporary frame using C-clamps to maintain vertical alignments (Figure 5-13). The photo electric gate was then attached to an adjustable height table and the plywood and sorbothane impact pad placed beneath the impact point of the rammer.

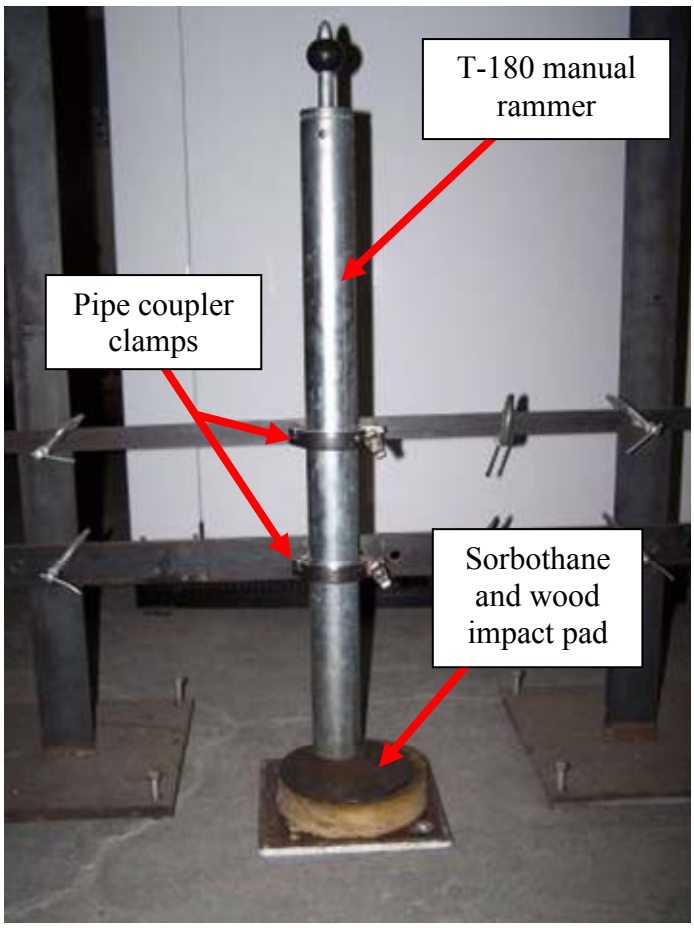

Figure 5-13. Frame for maintaining vertical alignment of rammer.

The adjustment described for the mechanical compactor was performed for this setup as well, i.e., the sensors were set such that the rammer was located just beyond the switching point. The mean of at least 25 impacts were then recorded for each of the six manual T-180 rammers. These six means were then summarized by their mean and variance, 14.25 ft-lb and 0.005 ft^2-lb^2, respectively, and then used to perform a bootstrap procedure to ensure sufficient tests were conducted. The bootstrap mean was calculated as 14.25 ft-lb as well, with the mean variance of the bootstraps determined to be 0.004 ft^2-lb^2. The most probable reason why the theoretical energy of 15 ft-lb (10 lb x 1.5 ft drop height) was not achieved is due to friction between the rammer and hammer housing. It is virtually impossible to provide a friction free fall since even a

slight inclination of the hammer will create concomitant friction between the moving mass and its housing.

Of significant importance with the bootstrap procedure is the variance determined to be on the order of 6×10^{-6}, which suggests that the calculation of the bootstrap means is highly precise. This high precision indicates that six values for the energy associated with the manual compaction rammer is a sufficiently large population to accurately determine the mean and variance to describe the population of all T-180 manual rammers. The small variance suggests that for any manual rammer, the energy is likely to be extremely close to 14.25 ft-lb.

5.3.3 Base Compliance

Following the measurement of the kinetic energy for each of the machines tested at the sixteen compaction labs, force and acceleration at the base plate were measured for multiple impacts of the rammer (three to eight) on each machine in the population using the base compliance instrumentation (Figure 5-5). The mean force and acceleration for each machine were plotted and reflect similarly to each other for any given machine (Figures 5-14 and 5-15), machines with a high mean force display high mean accelerations. The standard deviations are relatively low compared to the magnitudes, although there are four types of base systems in the population and measurements are also a function of velocity.

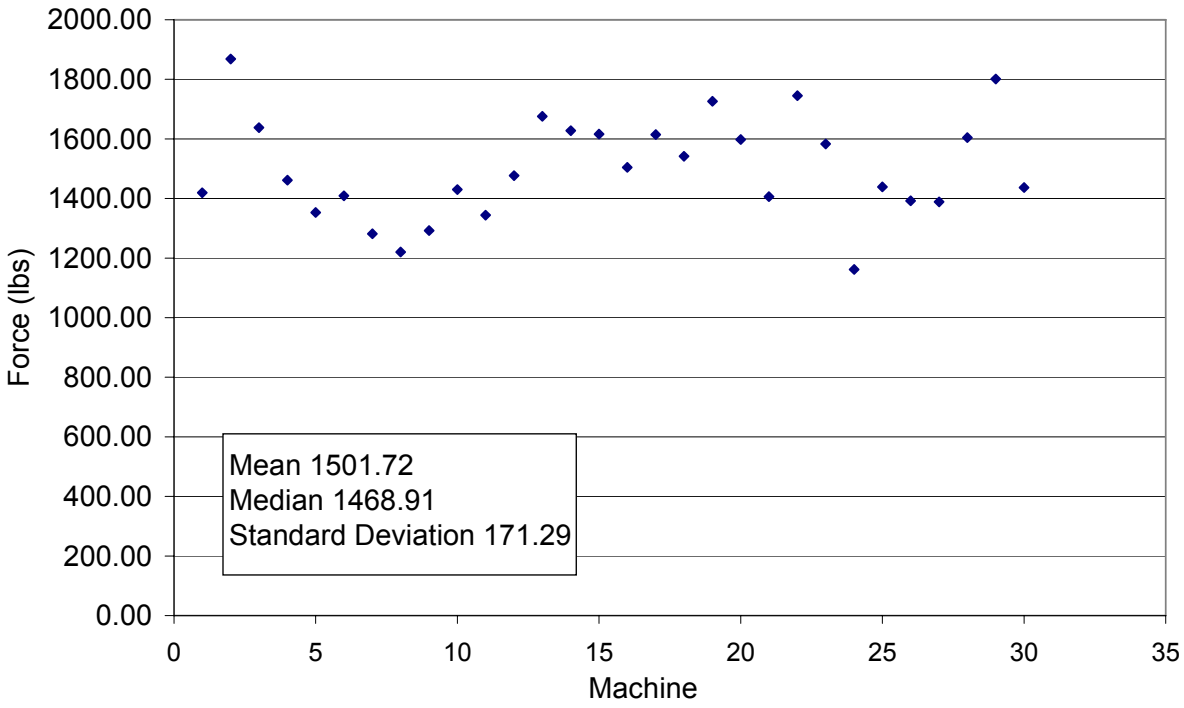

Figure 5-14. Scatter plot of average maximum force.

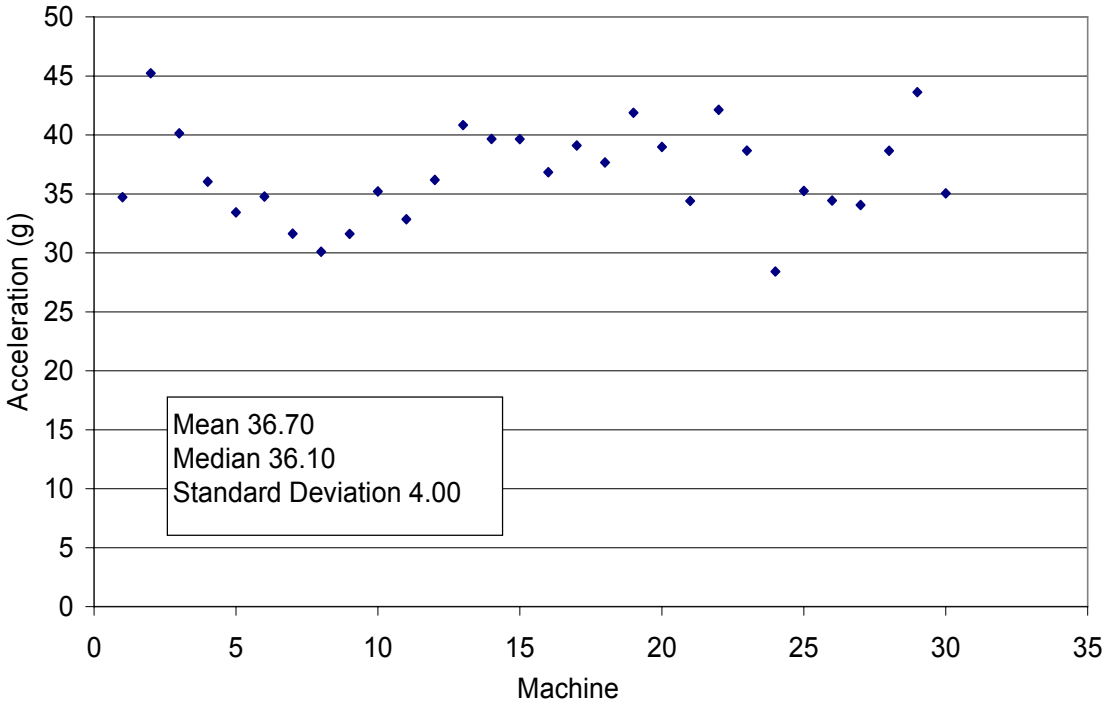

Figure 5-15. Scatter plot of average maximum acceleration.

The primary reason for measuring the force and acceleration at the base of the compaction equipment was to quantify the energy or the purpose of identifying a possible source of difference in compaction density results. As previously discussed, the stiffness of the material supporting material beneath the compaction mold has an influence on the resulting maximum dry density and optimum moisture content.

5.3.4 Force Compressive Energy Theory

In an effort to quantify the effect that different base types have on the compaction process, the energy at the base of the compaction device needed to be quantified. Compressive energy at a point along a Standard Penetration Test (SPT) rod can be expressed as an integral of the force squared with respect to time multiplied by the dynamic impedance of the SPT rod (Palacios 1977) (Equations 5-1 and 5-2). In the case of the load cell being the same cylindrical shape and displaying 1-D wave transmission down the length of the cylinder (the load cell housing in this case), the same assumptions hold true and validate the use of SPT compressive energy equations in this study.

$$\text{Dynamic Impedence} = \frac{c}{Ma} \tag{5-1}$$

$$\text{Energy}_{\text{impact}} = \frac{c}{Ma}\int_0^t F_i^2 \tag{5-2}$$

C = wave velocity (ft./sec)
M = Young's Modulus (psf)
a = cross sectional area ($ft.^2$).

5.3.5 Compressive Energy Results

For each machine, a numeric integral of the force squared was calculated for the time over which it occurred. The mean of the integrals were then recorded for each machine (Table B-2).

Force and acceleration were plotted for several machines and used to verify that the dynamic impedance of the base compliance system was the same for every machine (Figure 5-16). The relationship of measured force to acceleration of the system was observed to be linear. This relationship verifies that the dynamic impedance for the system is a constant value.

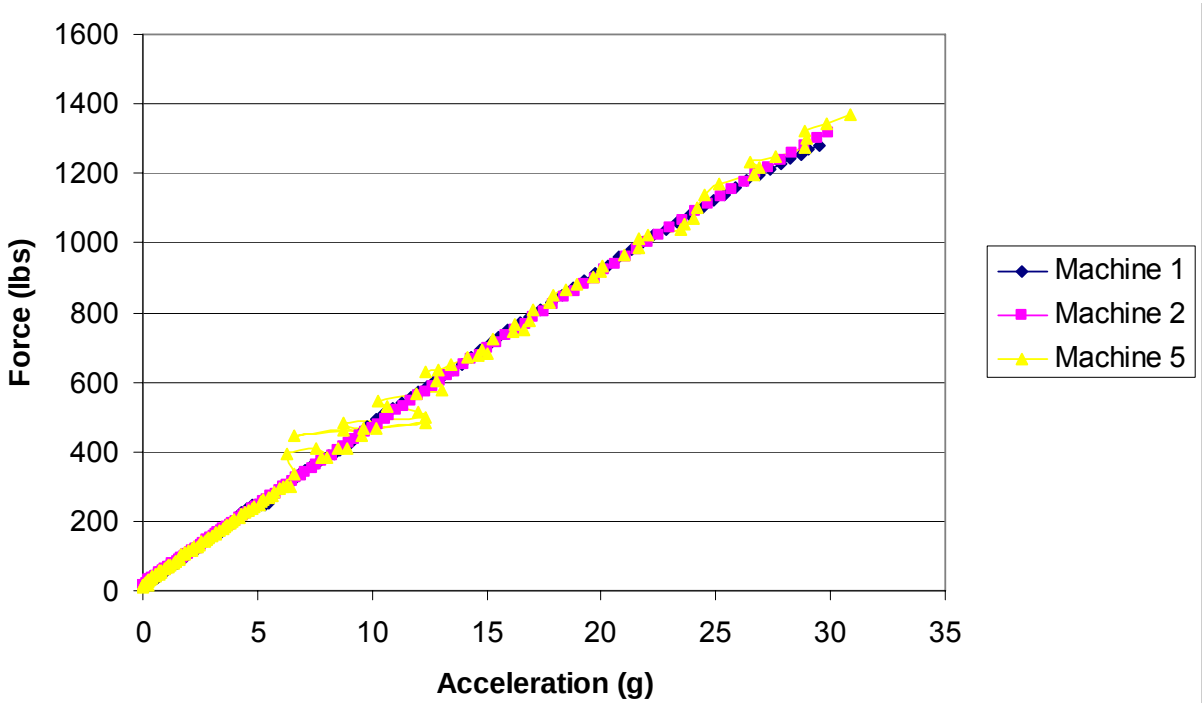

Figure 5-16. Dynamic force and acceleration.

Since this relationship is linear the dynamic impedance of the system can be determined by dividing the particle velocity occurring at a point in time by the dynamic force measure at the same point in time (Equation 5-3). Since the accelerometer was mounted on the same surface and close to the load cell, the acceleration record is useful in determining the particle velocity at times corresponding to force measurements.

$$\text{Dynamic Impedance} = \frac{V}{F} \tag{5-3}$$

F = Force (lbs)
V = Velocity ($A \times g \times t$) (ft/sec)
g = Gravitational constant (32.2 ft/sec^2)
t = Time (sec)

Values were pulled from figures 5-14 and 5-15 for typical maximum forces and accelerations from T-180B machines and used to evaluate Equation 5-3. A typical dynamic force of 1500 lbs and an acceleration of 37 g were used to evaluate the equation using a time of 0.00375 sec. Calculation of the particle velocity yields 4.5 ft/sec, resulting in a calculated dynamic impedance of 0.003. This illustrates that a value on the order of 1/300 ft/(sec-lb) accurately assesses the dynamic impedance of the base compliance device and the base system for T-180B machines.

It has been illustrated that the force and acceleration relationship for the machines tested was constant and the dynamic impedance of the base system evaluated. Therefore, the use of the accelerometer is not required for determination of the compressive energy on an individual machine basis.

Due to the difference in the wave transmission through the different sized compaction mold base plates required for the T-180A and T-180B tests (4 inch and 6 inch diameter molds), the sample population of base compliance data was subdivided by base type for further analysis. This resulted in a subpopulation of nine T-180A machines and twenty-one T-180B machines. The subpopulation of the T-180A machines was too small to be used in further calculations.

Of the twenty-one T-180B machines, several different base types were represented. These consisted of two machines with plywood mounted between the machine and the foundation block, three machines mounted directly to concrete, and the remaining sixteen machines were

mounted with aluminum spacers or steel nuts between the machine and their foundation blocks. The integral of the force squared as well as the maximum force and maximum accelerations for machines mounted with plywood displayed uncharacteristically high compliance measurements. Due to this unrepresentative behavior and uncommon occurrence in the population (two machines), they were removed from the final analysis so as to not misrepresent the sample population of T-180B compaction machines.

Summary statistics were performed on the compressive energies of the nineteen machines as well as a bootstrap procedure to ensure that the population of nineteen machines was adequate for quantifying the variance of the population. A summary table containing the measurements from the nineteen machines is presented in Table B-2 in Appendix B. The mean compressive energy was 11.66 ft-lb with a variance 1.39 $(\text{ft-lb})^2$ and the mean of the bootstrap means was 11.65 ft-lb and variance mean of the bootstraps equal to 1.32 $(\text{ft-lb})^2$. The variance of the bootstrap variances was then calculated as 0.082, more than two orders of magnitude smaller than the variance of the sample, thus indicating that nineteen machines is large enough to establish the mean and variance of the population of T-180B base compliances. The coefficient of variation (COV or CV defined in Equation 5-4) was then calculated for both the sample and bootstrap populations, and were found to be in good agreement, i.e., 0.12 and 0.11, respectively.

$$\text{COV or CV} = \sigma/\mu \tag{5-4}$$

σ = standard deviation
μ = mean.

5.4 Measured and Predicted Dry Density Variance of A2-4 Soil

5.4.1 Background

As identified earlier, soil compaction is affected by the amount of energy imparted to the soil sample, the stiffness of the base on which the sample is compacted as well as the moisture

content of the sample being compacted and other operator influences. Examples of operator influences are mixing of soil, placement and thickness of lifts as well as placement of mold in frame (i.e. tightening of bolts). Of interest, is the relative influence of each variable on the resulting dry densities as measured after compaction. The latter effects may readily be assessed by establishing a linear relationship between dry density, moisture, kinetic energy, and compliance and then assessing the variance of the relationship. Subsequently, if the measured kinetic or compliance variance were substituted into the linear variance relationship, a variance of the dry density may be predicted. Reasons why the predicted variance may not agree with the measured variance is that the relationship are; one the relationship may not be linear and two, operator effects. To ensure the relationship is linear, a small moisture content range should be considered on both the dry and wet side of optimum. In the case of operator influence, its variance is unknown. However, by comparing the expected that variance between the measured dry densities and predicted variance due to kinetic energy, compliance and moisture content, the difference may be assumed to be operator effects (i.e. lumping all other influences). In addition, the linear variance relationship will assist in identifying where improvements in compaction testing should be undertaken. The latter is very important, since current ASTM specifications require comparisons of dry densities between manual and automatic compaction equipment, and not necessarily the dependent variables (e.g. compliance stiffness). A discussion of soil selected, testing requirements, statistical analysis and results follows.

5.4.2 Properties of Test Soil

An A-2-4 embankment fill soil was selected for the soil density compaction study due to its prevalence in Florida and expected large range (vs. A-3 soil). A large sample of A-2-4 material was obtained from a Florida DOT borrow pit (Lake City) and tested at the SMO laboratory. The compaction results for T-180 are given in Figure 5-17, content from the FDOT

State Materials Office evident from Figure 5-17, the moisture vs. dry density curve is highly nonlinear. To assume it to be linear over a small range, the soil testing had to be broken up into two moisture ranges, if the study was to be performed on the whole compaction curve. Since there are different processes occurring on either side of optimum moisture, both should be tested. For instance on the wet side of optimum as more energy is imparted to the soil, the zero air void line is approached, this results in a maximum attainable dry density for any moisture content, causing lower variance in the overall density results. On the dry side, small energy changes usually result in larger density changes.

Consequently, moisture contents at 6 and 7.5 were selected for testing. Subsequently, samples of the test material were then distributed to several state and private labs and asked to assess dry densities at two moistures, one wet of optimum and the other dry of optimum.

STATE MATERIALS OFFICE SOILS LABORATORY	6" STANDARD LBR 6" MODIFIED	REVISED 12/05 BY: D.B.

PROJECT DESCRIPTION: U.F. SOIL DENSITY COMPACTION PROJECT
MATERIAL DESCRIPTION: TAN SAND/SOME CLAY BRANCH

LIMS		SOIL		DATA	
SAMPLE DATE:	10/17/2008	SOIL TYPE:	EMBANKMENT	LIQUID LIMIT:	
RECEIVE DATE:	10/17/2008	SOIL CLASS:	A-2-4	PLASTIC INDEX:	
LIMS NUMBER:		DATE COMPACTED:	10/28/2008	CARB. CONTENT:	
LAB. NUMBER:	23477	DATE TESTED:	10/30/2008	MAX. DENSITY:	134.8
SAMPLE NR:	S-1	TECHNICIAN:	TIM BLANTON	OPT. MOISTURE:	6.8%
MATERIAL NR:	004	TEST METHOD:	T-180 FM 5-515	LBR VALUE:	160.0
PIT NUMBER:					

DENSITY/ LBR CALCULATION:							11/25/2008	GRADATION:
Mold Number	86	153	106	208	218			PASS #3.5":
Water Added (%)	4%	5%	6%	7%	8%			PASS #3/4":
Wet Mass.& Mold(gm.)	11775	11901	12053	11980	11943			PASS #4: 100%
Wet Mass & Mold(lbs.)	25.96	26.24	26.57	26.41	26.33			PASS #200:
Mold Mass (lbs.)	15.84	15.80	15.82	15.61	15.61			
Wet Mass (lbs.)	10.12	10.44	10.75	10.80	10.72			NOTES:
Wet Unit Mass (lbs./ft3)	134.9	139.1	143.3	144.0	142.9			
Dry Unit Mass (lbs./ft.3)	129.3	132.1	134.5	134.1	132.1			
L.B.R.	73.0	102.0	160.0	111.0	56.0			
Record Number	15	14	13	12	11			
MOISTURE DETERMINATION:					Damp			
Can Number	121	119	63	61	11			
Wet Soil & Can(gm.)	644.3	673.2	642.8	699.3	681.7			
Dry Soil & Can(gm.)	620.9	643.3	608.5	656.3	635.8			
Water Mass (gm.)	23.4	29.9	34.3	43.0	45.9			
Can Mass (gm.)	76.7	77.0	81.6	75.4	76.4			
Dry Soil Mass (gm.)	544.2	566.3	526.9	580.9	559.4			
Moisture Content(%)	4.3	5.3	6.5	7.4	8.2			

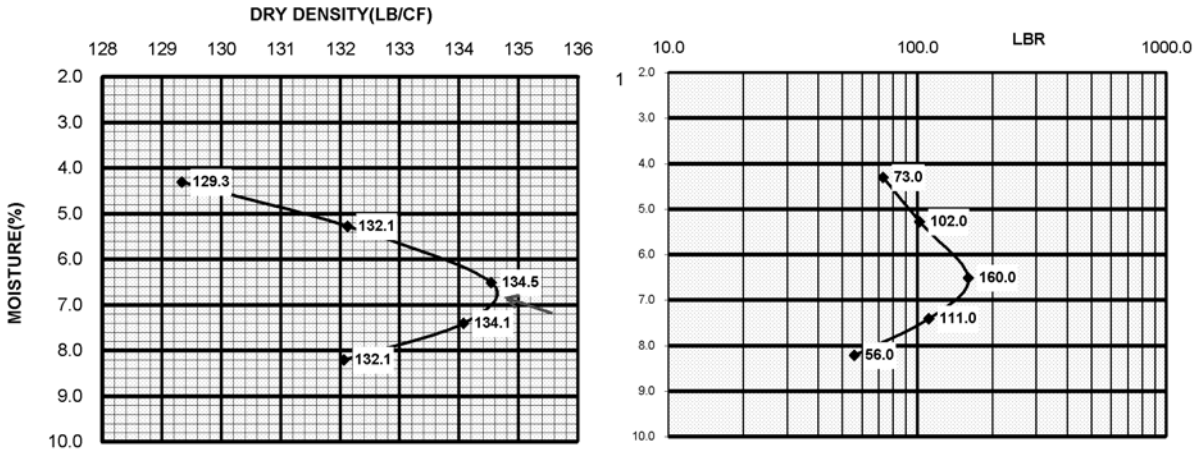

Figure 5-17. Soil compaction results of A-2-4 test material.

Each participating laboratory was then asked produced 20 soil density pills on specified T-180 machines without reconstituting the soil. In each test performed, the technician running the test was to use a portion of the sample large enough to prepare a pill, hydrate it to the specified moisture content and compact the pill as they would ordinarily do in accordance with AASHTO T-180 procedures. The use of a new sample of material for each pill was requested so as to preserve the structure of the soil and remove any error possibly associated with repeatedly drying and hydrating the soil.

Ten pills were compacted on the dry side of optimum at 6% moisture content and ten were compacted on the wet side of optimum at 7.5% moisture content (Figure 5-18).

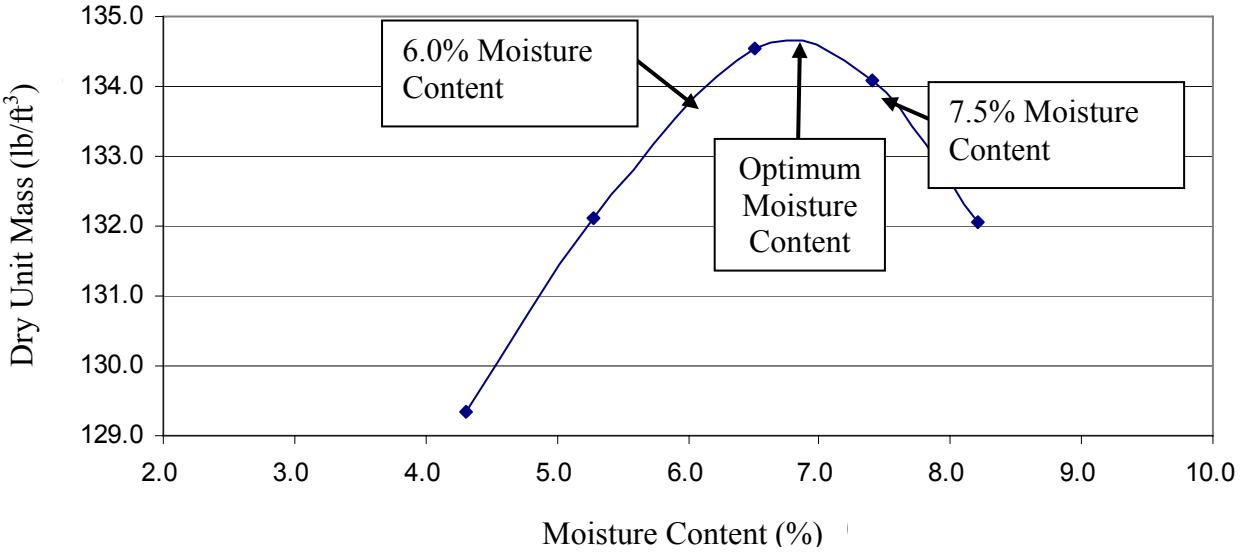

Figure 5-18. Test target moisture content on Proctor curve

In accordance with the AASHTO T-180 standard for soil compaction, the moisture content of each pill was determined by the machine operator utilizing an oven dried sample of the pill material.

A total of six machine test results were received back from the labs. Shown in Figures 5-19 and 5-20 are scatter plots the data obtained. Since each machine's results are identified, the variability of both machine and by labs are evident in Figures 5-19 and 5-20. Also, the plots

clearly depict the inability for testing to be performed at a single given moisture content as evident from the spread of data across a moisture content range. The latter spread occurred over different machines as well as from any single machine's test. In addition, some of the results, the moisture content of the tests were far from the specified testing moisture content and so these values were removed from the analysis so as to not invalidate the assumption of linearity. In addition, it should also be noted that the moistures reported are average values and do not consider any variability within the pill.

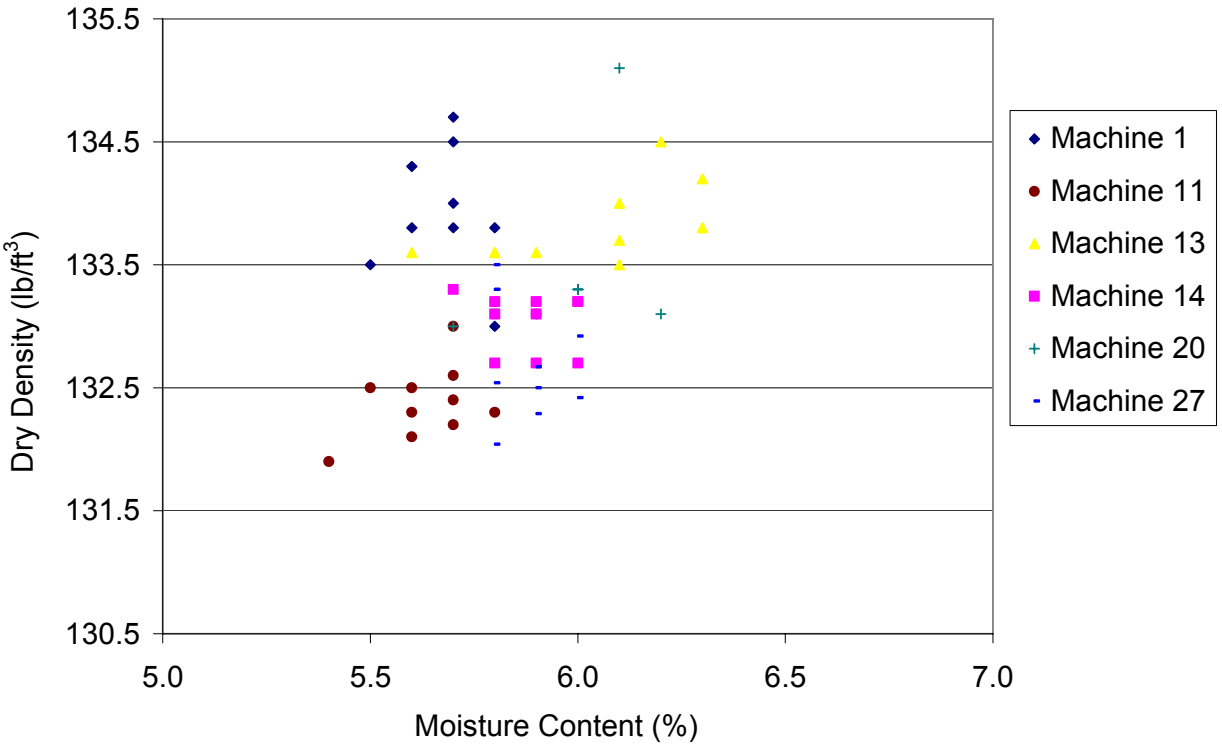

Figure 5-19. Scatter plot of 6% moisture content results.

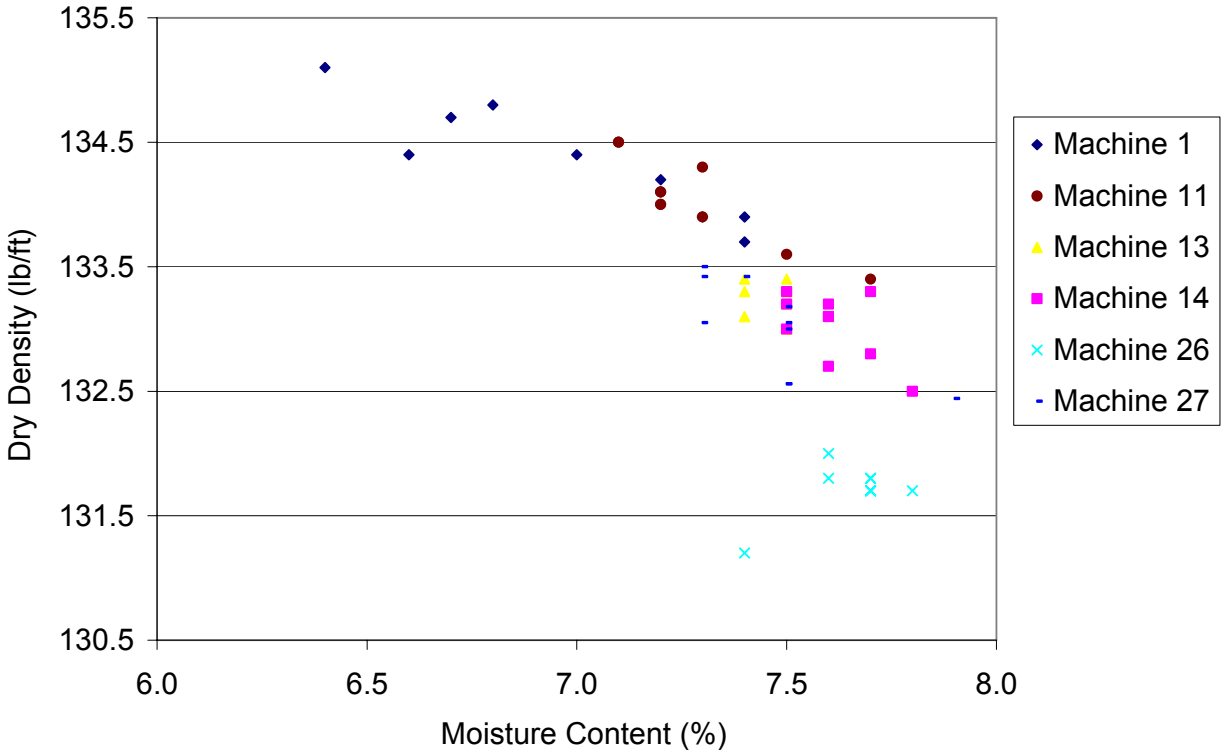

Figure 5-20. Scatter plot of 7.5% moisture content results.

5.4.3 Regression Analysis of Lab Test Results

As identified earlier, a linear relationship between dry density with moisture, kinetic energy and base compliance , Equation 5-5 was assumed:

$$\gamma_d = A(\omega) + B(KineticEnergy) + C(BaseCompliance) + D \qquad (5\text{-}5)$$

In order to prepare the data for analysis the results from the density testing performed on T-180B machines were subsequently paired by mean kinetic energy and base compliance (Tables B.4 and B.5) in order to establish the constant coefficients in Equation 5.5. The Summary data tables (Tables B.4 and B.5) were then used to calculate a regression equation by utilizing the least squares method of analysis from the MiniTab software.

The following linear equations describe the dry density as a function of moisture content, kinetic energy and compliance for the 6% and 7.5% moisture content portions of the compaction curve, respectively (Equations 5-6 and 5-7).

$$\gamma_d = 0.846 \times \omega + 0.007 \times KE + 0.489 \times CE + 122 \tag{5-6}$$

$$\gamma_d = -2.05 \times \omega + 0.202 \times KE + 0.187 \times CE + 144 \tag{5-7}$$

ω = moisture content (%)
KE = Kinetic Energy (ft-lbs)
CE = Base Compliance Energy (ft-lbs)

The evaluation of each of these equations using the mean of each variable illustrates the ability of the equations in determining the expected values of dry density. For example, Equation 5-6 was evaluated using the mean moisture content of the "6%" moisture content data, mean kinetic energy and base compliance (Tables 5-1) for the six machines tested, and the predicted dry density was 132.7 pcf. When compared to the mean value of the measured dry densities used to generate this regression equation, a mean of 132.2 pcf was found. Evident, the regression equation does quite well in estimating the mean. In the case of 7.5% moisture content, and the measured kinetic, compliance (Table 5-2) and moisture content, the regression equation (Equation 5-7) predicted a dry density of 133.6 pcf. The actual measured mean dry density of the data is 133.2, or a difference of 0.4 pcf. Because of the good agreement between the expected dry density and the mean dry density, the variance of the densities on the wet and dry side may now be explored.

Table 5-1. Component Summary Table for Machines Used in "6%" Moisture Content Regression Analysis

Machine Number	Mean Kinetic Energy (ft-lb)	Compressive Energy (ft-lbs)
1	13.20	12.29
11	13.43	10.87
13	14.15	12.58
14	13.92	11.31
20	14.15	10.35
27	13.75	11.55
Variance	0.15	0.71
Mean	13.77	11.49

Table 5-2. Component Summary Table for Machines Used in "7.5%" Moisture Content Regression Analysis

Machine Number	Mean Kinetic Energy (ft-lb)	Compressive Energy (ft-lbs)
1	13.20	12.29
11	13.43	10.87
13	14.15	12.58
14	13.92	11.31
26	12.22	8.56
27	13.75	11.55
Variance	0.48	2.07
Mean	13.44	11.19

5.4.4 Standardized Regression Equation

Since the units of each variable are not the same, the magnitude of the coefficients of each variable cannot be directly compared to determine which parameter has the most effect on the outcome. Because this is an issue of interest, a process of standardizing the data for each parameter was carried out. Standardization removes the effect of the mean and the variance on the determination of coefficients in the regression analysis (Equation 5-8).

$$z_i = \frac{(X_i - \mu)}{\sigma} \tag{5-8}$$

X_i = Original Variable Value
μ = Mean of Variable
σ = Standard Deviation of Variable
z_i = Standardized Variable

This process forces the mean of each of the variables to be zero and the variance to be one. The entirety of tables B.3 and B.4 were then standardized and used to generate a standardized regression equation for the each of the moisture contents at 6% and 7.5% respectively (Equations 5-9 and 5-10).

$$\gamma_{dStd} = 0.235 \times \omega_{Std} + 0.004 \times KE_{Std} + 0.572 \times CE_{Std} - 0.071 \tag{5-9}$$

$$\gamma_{dStd} = -0.679 \times \omega_{Std} + 0.152 \times KE_{Std} + 0.293 \times CE_{Std} - 0.0012 \tag{5-10}$$

From this standardization analysis, it can be noted that in terms of direct effect on the resulting dry density without the effect of units, base compliance energy has the greatest influence on results at 6% moisture content (Equation 5-9). It is shown that kinetic energy has almost no discernable effect on the resulting dry density at 6% moisture. The latter may be attributed to the small coefficient in Equation 5-6 for the Kinetic energy which was an outcome of the machines that data was recorded, i.e. very small variance of KE and constant, mean. Generally, the kinetic energy has a large effect on density, i.e. T-99 vs. T-180. If more machines were used to determine the regression equation it is likely that a more discernable trend would occur, resulting in a larger coefficient. For the analysis of the 7.5% moisture content, Equation 5-7, it is evident that the standardized base compliance had the largest effect on resulting densities. In the non-standardized form, the kinetic energy has the largest effect on the resulting

dry density. This is directly related to the fact that the measured values of kinetic energy are larger than those of base compliance and the standard deviation is smaller on the sub population of kinetic energies. While the standardized regression equation is of value, the more useful of the regression equations is the non-standardized form, which allows an analysis of the variance of each of the parameters and the variance of the resulting dry densities.

5.4.5 Variance of Dry Densities, Measured vs. Predicted

Application of the second central moment to the coefficients of the mean equations (Equations 5-6 & 5-7) allows the variances of each parameter to be summed to find the expected variance of the resulting dry densities (Equation 5-11). Note, the variance of the constant "D" in the regression Equation (5-5), is zero, which leaves the sum of the component variances (Tables 5-1 & 5-2) times the square of each of their corresponding coefficients.

$$Var(\gamma_d) = A^2 \times Var(\omega) + B^2 \times Var(KineticEnergy) + C^2 \times Var(BaseCompliance) \quad (5\text{-}11)$$

The Variance form of the regression analysis equation, Equation 5-11 is particularly useful for determining the effect that a parameter's variance has on the expected variance of the outcome. For instance, when the variance of the moisture content, kinetic energies (Tables 5-1 &5-2) and the base compliance (Table 5-1 &5-2) energies are used to evaluate Equation 5-11 this will result in a value for the expected variance in the resulting dry densities. For instance, the predicted variance of dry density for the tests performed at 6% moisture is 0.20 $(pcf)^2$. Where as the actual measured variance of the dry densities recorded from the six laboratory tests was 0.52 $(pcf)^2$. This shows the ability to account for the cause and magnitude of nearly half of the variance observed in density results. Carrying out the same approach with data from the 7.5% moisture results, the predicted variance in the dry density is 0.48 $(pcf)^2$. The measured variance of laboratory data at 7.5% moisture was 0.84 $(pcf)^2$.

The observed differences in the measured and calculated variances of the dry densities are likely due to the operator of the machines effect on the dry density results. This effect cannot currently be completely quantified due to the complexities in the evaluation human ability. Some of the sources of possible variance that can be attributed to the operator are:

- -Variances in the process of mixing the soil and water
- -Lift Thickness
- -Amount of tamping applied to the specimen prior to compacting each lift
- -How tightly the compaction mold is assembled
- -Variance in sampling to determine moisture content of the pill
- -Accuracy in trimming final lift from the top of the compaction mold

5.4.6 Summary of Predicted and Measured Variances of A2-4 Tested Soil

The developed regression equations for mean and variance of dry density vs. moisture content, kinetic energy and compliance can only be interpreted to be representative of the machines used to generate the equations. If more data is used to generate the regression equations, a change in the coefficients of the terms in the equation may occur. Similar changes would occur if different soils were tested. However, for the sake of interest in what type of results might be acquired from the possibility that the regression equations are representative of the entire population of machines, the variance of the population of thirty kinetic energies (0.45) and nineteen T-180 base compliance measurements (1.39) were used in the variance Equation 5-10, an expect variances of 0.36 $(pcf)^2$ at 6% moisture content and 0.45 $(pcf)^2$ would be computed for 7.5% moisture. Interestingly, 7.5% moisture content variance agrees quite closely with the variance recorded for the 6 machine results in this study. The latter suggests that more machine tests need to be performed on the dry side and especially with different kinetic energies. Also from a comparison of the measured and predicted variances of the machines tested significant variance (i.e. 50%) may be attributed to human operator differences.

CHAPTER 6
CONCLUSION/RECOMMENDATIONS

6.1 Conclusions

6.1.1 Background

Laboratory Proctor compaction is performed by state agencies and private laboratories for determination of unique dry density-moisture content relationship of soils used for embankment construction. This type of compaction is preformed through imparting the kinetic energy, to a confined soil mass, of a standard rammer mass falling from a standard height (AASHTO T-99, T-180 and ASTM D689, D1557).

For quality control of Proctor compaction through out the state of Florida, the Florida Department of Transportations State Materials Office (FDOT-SMO) routinely compares compaction results, i.e., maximum dry density, from mechanical compactors. This, indirectly, assess calibration, or compliance, of the compactor that undergoes a standard calibration (ASTM D2168) based on obtaining similar maximum dry densities, within tolerance, between the manual and mechanical Proctor compaction process. The dry densities obtained using the compactors are influenced by the kinetic energy available, the base that the machine rests (foundation and cushion), and the operator. Variance of these parts will lead to, perhaps, unsatisfactory variance in the densities and without quantifying the variance of each part compactors may be out of calibration according to standards.

The objective of this research was to develop a portable, electronic calibration device for use on mechanical Proctor compaction machines and determine sources of variance in soil density results. The Portable Dynamic Energy Calibrator (PDEC) was developed and used to quantify the kinetic energy and the compressive impact energy on T-180 mechanical compaction machines throughout central and north Florida. Variance in soil densities was quantified for six

of T-180 machines so as to quantify the operator influence and variance. The results provided valuable insight into the variability of compaction machines, both individually and as a population, and the effect of their parameters on soil density. It is expected that the FDOT will continue to use this equipment in the future to verify that compaction machines are in compliance with appropriate standards (AASHTO T-180 and ASTM D1557). A summary of major findings in each category follows.

6.1.2 Calibrator Development and Operation

The calibrator was developed to capture the rammer's kinetic energy at impact and the compressive force from rammer impact at the compactor base. Portability and rapid employment was a necessity throughout the development as compactors throughout the state will be observed. Data collected and stored on a notebook computer can then be processed through a macro command with in an Excel spreadsheet allowing the user to immediately observe results.

A photo electric gate (Figure 6-1) was developed to be attached to the top of the compaction machine and capture the passing rammer rod (Figure 6-2). Validation and determination of accuracy consisted of a laser displacement sensor companion observation of the rammer and rod during operation. It was determined that velocities measured using the photo gate are representative of the rammer's impact velocity and used in kinetic energy calculation with an accuracy of ± 1%. After the photo electric gate captures the rammer impact velocity, the user determines the rammer mass and enters into the spreadsheet for calculation of the kinetic energy. Since the operation of the machine consists of the rammer rotating about a point, a complete rotation is observed allowing for multiple kinetic energy values to be calculated.

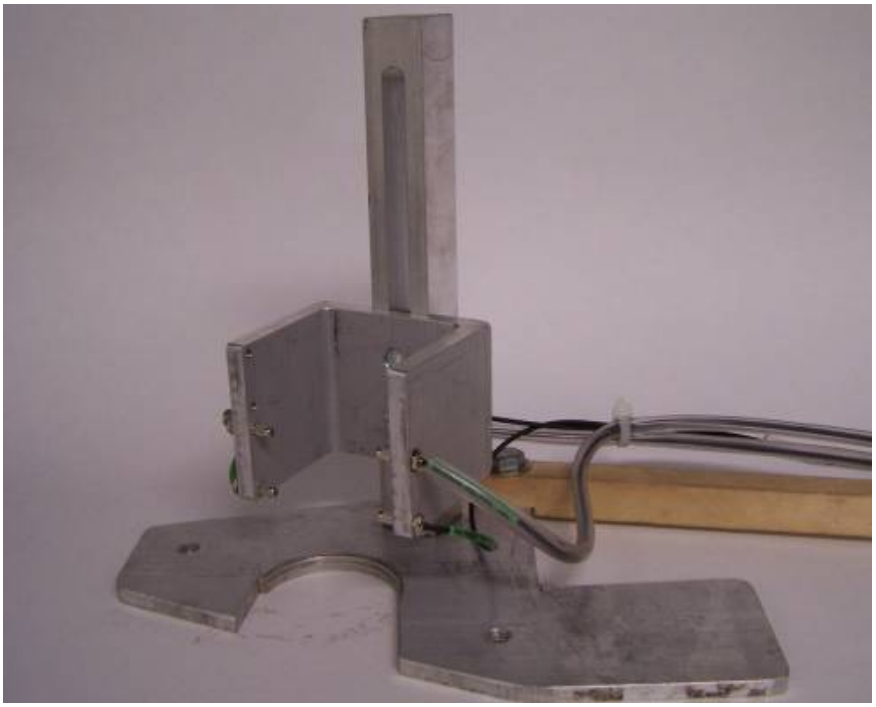

Figure 6-1. Photo electric gate.

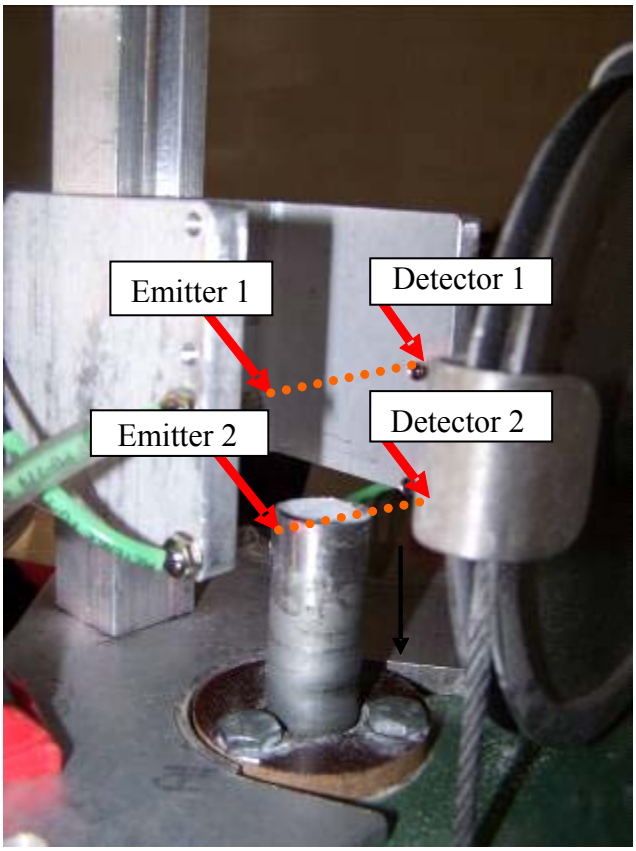

Figure 6-2. Photo electric gate on compactor.

It was shown that the base system, i.e., foundation and cushion (Figure 6-3), influence the compressive energies and thereby the maximum dry densities and optimum moisture content (Figure 6-4). This is due to the differences in the modulus and density of the two base systems. The velocity, c, of a compressive wave is a function of materials modulus and density. A dynamic load cell rigidly to a compaction mold plate (Figure 6-5) and placed at the base of the compaction machine is able to capture the impact compressive force. By integrating the impact force over the event duration ($t_2 - t_1$) and multiplying by material dynamic impedance (Equation 6-1), the compressive energy from an impact can be determined (Equation 6-2).

$$\text{Dynamic Impedence} = \frac{c}{Ma} \tag{6-1}$$

$$\text{Energy}_{\text{impact}} = \frac{c}{Ma}\int_0^t F_i^2 \tag{6-2}$$

c = wave velocity $\sqrt{(M/\rho)}$ (in/sec)
M = Young's Modulus (psi)
A = cross sectional area (in^2)

The use of the dynamic load cell on machines within the population is valuable in that it allows for comparison between machines and its influence on the density results.

The compressive force measurement device is fixed into position at the compactor base and a series of impacts (5-10) are captured. Since the device does not rotate as does the rammer, the machine must be operated on single blows. This requires placement of the rammer off center to the load cell such that upon lift and rotation the rammer strikes the center of the load cell. Next, the user enters the impedance into the spreadsheet and keystrokes the macro for calculation of the compressive energy.

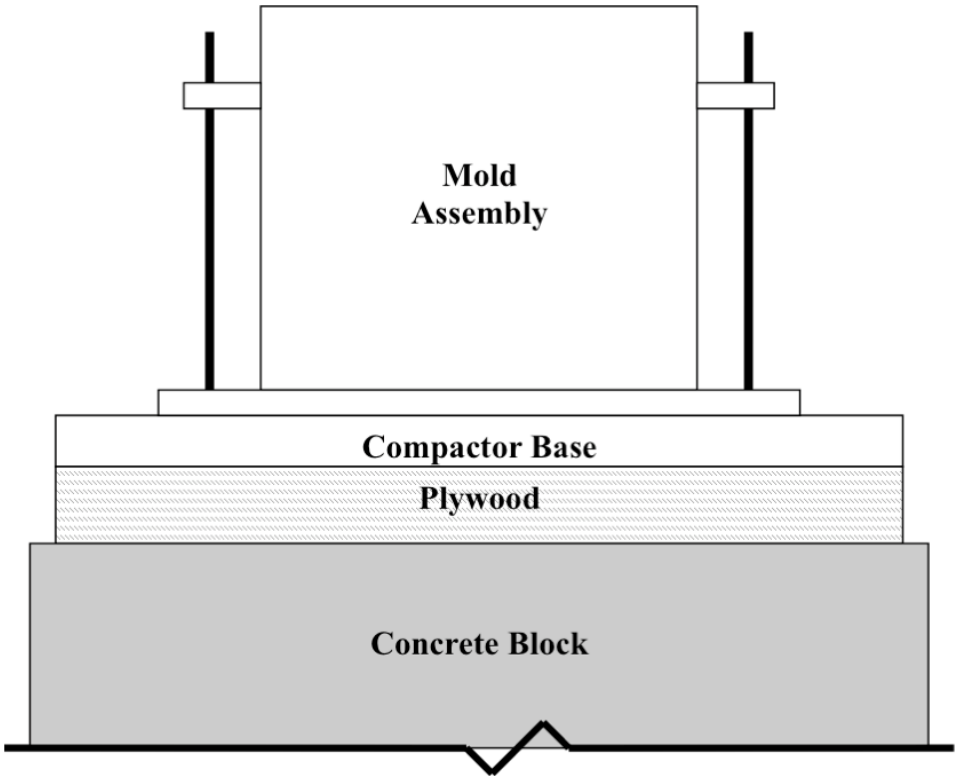

Figure 6-3. Compactor base configuration and mold assembly.

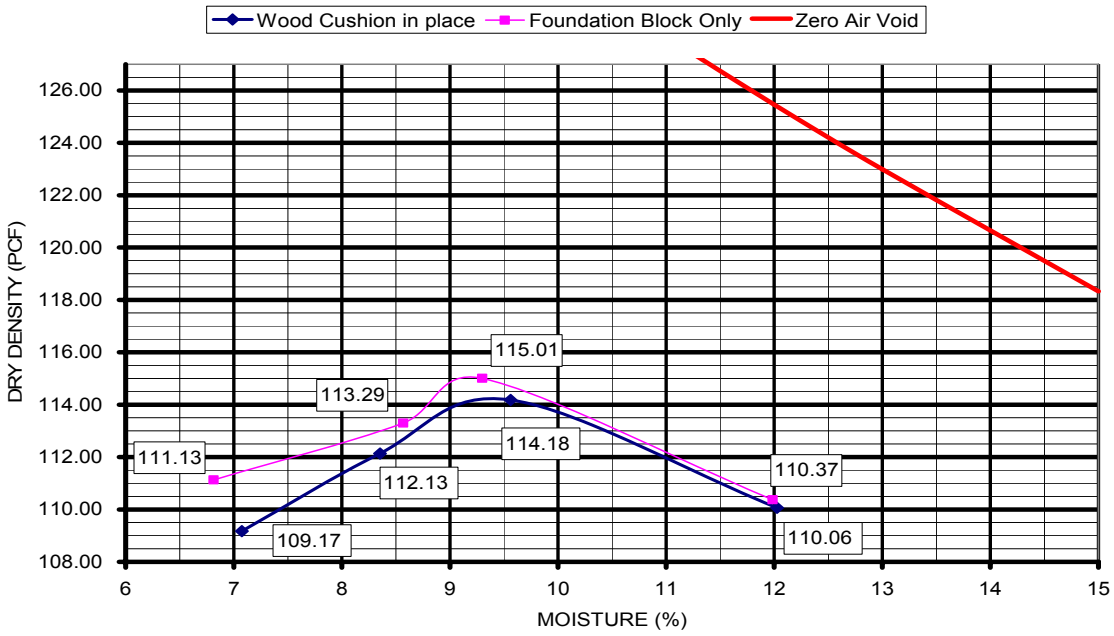

Figure 6-4. Influence of cushion on A-2-4 compaction curve.

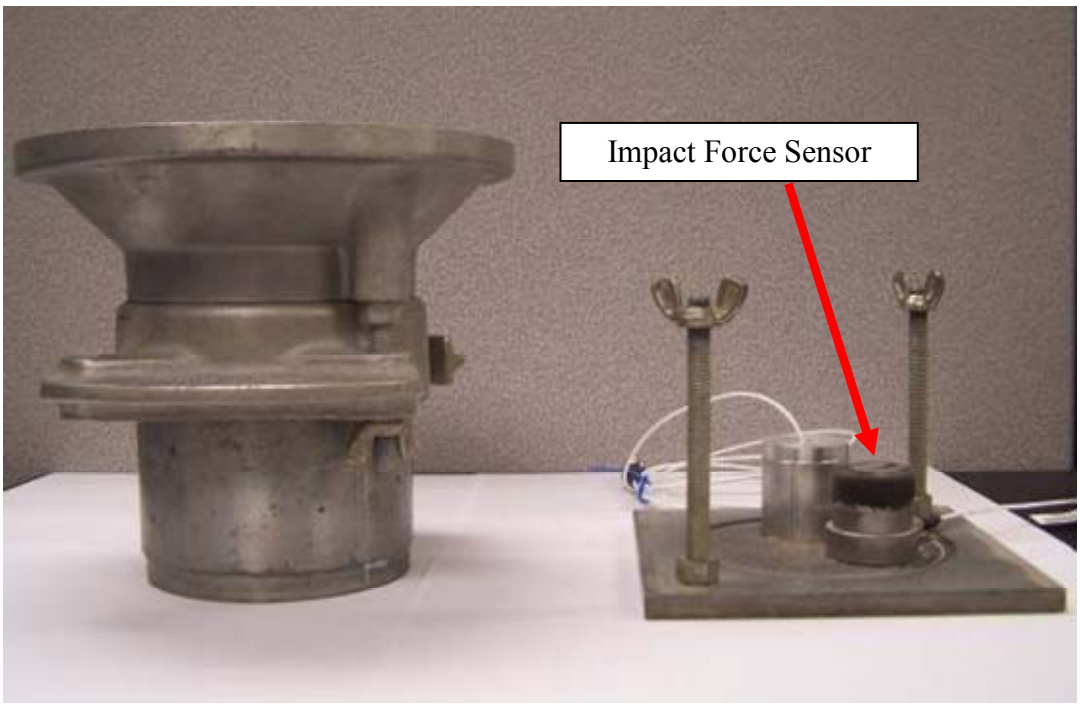

Figure 6-5. Instrumented mold assembly.

The Portable Dynamic Energy Calibrator (PDEC) is easily transportable and can be readily employed in a compaction laboratory. The photo electric gate is adjustable and affixes to the top of the compaction machine with no alterations needed to the machine. The dynamic force device is placed in the compactor and captures single rammer blows. A data acquisition system, which accompanies the devices, samples the sensors and stores the data for immediate analysis. The user can run a macro on the data collected and, with a few variables entered, can observe the rammer kinetic energy and base compressive energy.

6.1.3 Laboratory Testing and Data Analysis

6.1.3.1 Kinetic Energy

Sixteen state and private laboratories were tested with the PDEC for the quantification of energy their machines display. Thirty T-180 machines were tested for kinetic energy by monitoring a single rotation of the compaction hammer. Each machines tested displayed an energy less than the theoretical energy prescribed by AASHTO for T-180 soil testing. The

laboratory testing results also indicated that there is a well defined proportionality to the mean and standard deviation. Machines that display high variances in kinetic energy also display lower than normal mean kinetic energies. The population of machines tested displayed a mean kinetic energy of 13.66 ft-lbs with a variance of 0.45 ft^2-lbs^2.

Kinetic energy was measured for six manual T-180 compaction hammers, each hammer displayed nearly identical mean kinetic energies (14.25 ft-lbs) and variance (0.005 ft^2-lbs^2). This low variance of the mean kinetic energy indicates that all manual compaction hammers are essentially the same.

6.1.3.2 Base Compliance Energy

Due to the small population size, 21 T-180B machines with many base types, it was found that the mean and variance of base compliance energy could not accurately be assessed for any specific base type. However, it was determined that the population of machine base compliances was large enough to be analyzed as a whole for T-180B machines. The population mean of T-180B base compliance energies was found to be 11.66 ft-lbs and the variance 1.39 ft^2-lbs^2. Using this analysis it was found that the COV of the compressive energy (0.12) of the compaction machine was much larger than COV the kinetic energy (0.05).

6.1.3.3 Regression Analysis

Soil density results in conjunction with energy measurements from six machines were used to determine regression models that describe the effects of dependent variables on dry density at moisture contents wet and dry of optimum (Equations 5-6 & 5-7). The models were validated by calculating a predicted mean dry density that compared closely to the mean density of the laboratory tests.

The regression equations developed were used to determine the effect of each parameters variance on the variance of the reported soil densities. In the cases of tests run both wet and dry

of optimum the sum of the parameters variances were able to quantify approximately half of the total variance observed in density results. Base compliance contributes more variance to the resulting densities than kinetic energy. This was largely due to the larger variance observed in the base compliance measurements used to develop the regression equations. The remaining variance that cannot be quantified through summing measured variances of the regression parameters are likely attributed to the operator and any issues associated with the fit of the regression equation.

6.2 Recommendations

Current Proctor compaction calibration procedures do not quantify the parts of system (kinetic energy, base compressive energy, operator) which directly influence the density results. The regression analysis strongly supports identifying the sources of variability in resulting densities. It is highly recommended that a large scale testing procedure be carried out. This should involve the following:

- All machines be tested with the base compliance and kinetic energy devices
- Other soil types, i.e., A3 and A-1-b, be tested for influence of soil type
- Soil compacted at moisture contents wet, dry and possibly at optimum
- Technicians practice greater quality control over the determination of moisture

A low variance in moisture content during the testing procedure would allow the regression analysis to better determine the effects of the kinetic and base compliance energies on resulting dry densities.

The findings also support that control be exercised over the base system. A universal cement block and mounting configuration would help to minimize the variance of base compressive forces in the population and potentially negate the need for base compliance energy measurement in the future. As has been observed in this study the variance of base compliance energies is a large contributor to the dry density variance.

Following future regression testing, it is recommended, a threshold value for the mean kinetic energy and variance of the kinetic energy for individual machines be established. If a machine falls outside of this boundary, it may be necessary to adjust, service or replace parts on the machine.

APPENDIX A
OPERATION OF INSTRUMENTATION

The following steps are critical to the functionality of the Portable Electronic Calibration Device.

The Photo Electric Gate

- Assemble the guide post and base plate of the photo electric gate. The opening in the guide post is perpendicular to the leading edge of the base plate.
- Remove the thumb bolts from the "C" channel containing the photo electric sensors.
- Place the "C" channel on the guide post such that the line of sight of the photo electric sensors is parallel to the base plate's leading edge. The orientation of the "C" channel should be such that the photo electrics are on the bottom side of the "C" channel. Refer to the "C" channel for determining top/bottom of channel for proper orientation.
- Thread the thumb screws through the guide post and into the back of the "C" channel and lightly tighten.
- Mount the photo electric assembly on the compaction machine such that the rammer guide rod and guide rod bushing fall within the radius cut in the base plate and the base plate is clear of all moving parts.
- Use quick connection clamps to fasten the base plate to the top plate of the compaction machine. Making certain the clamps used for mounting will not interfere with the moving parts of the compaction machine.
- Check the rotational alignment of the photo electric sensors to ensure that the guide post is in proper orientation such that the lenses of the photo electric sensors will not be struck by the rammer rod.
- Turn on laptop and insert the USB cable for the measurement computing Data Acquisition system into any USB port on the laptop.
- Turn on power strip in instrumentation box.
- Allow sufficient time for data acquisition system and instrumentation to warm up and stabilize approximately 20 minutes.
- In the mean time select the appropriate size impact pad for the machine configuration to be tested. Place the impact pad on the compaction machines base and clamp in place using the mold clamp for the machine.
    - Note: Two impact pads have been provided and have been adequate for the testing performed by the University of Florida. The purpose of the impact pad is to provide a safe surface for impact of the rammer and dampen the blow of the

rammer such that the rammer is in at rest before being lifted by the grabber. Should a particular machine display instances in which the rammer is picked up by the grabber during a bounce, following the previous impact changes to the impact pad must be made to eliminate this effect. However the impact pad should have sufficient rigidity such that there is little deflection or deformation when the rammer is at rest on the surface of the impact pad.

- Place the rammer face on the impact pad.
- From the top of the machine adjust the vertical alignment of the "C" channel. The line of sight of the bottom pair of sensors should be just slightly above the top of the rammer rod so that the time of impact can be recorded. The switching threshold can be observed by watching the lights on the photo electric amplifiers change from green to red. Lift the rammer rod slightly to ensure that the amplifier switches in all orientations of the rammer this will ensure that the impact energy can be measured for all impacts.
- From the desktop of the provided laptop open TracerDAQ Pro.
- With "Strip Chart" selected from the list of options click "Run".
- On the file menu select "load configuration" and choose named configuration select "Kinetic Energy."
- Make certain the fiber optic cables of the instrumentation stay clear of the rammer and grabber assembly during monitoring.
- Select the "Play" button on the top of the screen. This will begin the acquisition of data from the photo electrics.
- Turn the compaction machine to the on position and record one complete revolution of the rammer.
- Once the rotation is complete switch the compaction machine off.
- Select the "Stop" to end the acquisition of data.

Saving and Importing Data into Excel

- From the file menu of TracerDAQ Pro select "Save As."
- Change the file type to ".txt" and save the record of impacts in the directory of your choice.
- From the desktop open Microsoft Excel 2003.

- From the file menu, select “Open.” On the File type drop down select “All Files.” Navigate to the file that was just recorded, select it and choose “Open.”
- The “Import Text Wizard” will be opened within excel, select delimitated and choose “Next.”
- Select “Comma” as a delimiter and click “Next.”
- Click “Finished.”
- Now The Data is ready for automated processing.

Kinetic Energy Processing

- On the keyboard of the laptop press the control key and the “k” at the same time.
- Fill in the cell requiring the mass of the rammer after verifying its mass.
- Table generated now displays the kinetic energy of each impact of the rammer.
- If a Boostrap of the kinetic energy is desired, press the control key and “m”
- The photo electric sensors can now be removed from the top of the compaction machinery.

Compliance Measurement Setup and Testing

- Connect the coaxial cable from the load cell on the compaction base plate to the PCB ICP.
- Turn on the PCB ICP.
- Allow the load cell and ICP to warm up and stabilize.
- Place the compaction mold into the compaction machinery and clamp in place using the base plate clamp for the machine.
- Align the rammer such that when the machine is switched on it will impact the load cell squarely on the impact surface. The resting height of the rammer face should be on the same horizontal plane as the face of the load cell and the grabber for the machine in its lowest point of travel and gripping the rammer rod.
- When the machine is switched on the rammer will begin to be lifted, rotate approximately 35-40 degrees and freefall. Attention to the location to the impact should be checked. Upon verifying the rammer will impact squarely testing is ready to be performed.

- On the File menu of TracerDAQ Pro select “Load Configuration,” choose named configuration, select “Base Compliance” to load.

- Once the configuration loads, select scan rate/ trigger settings and set the trigger ot begin acquisition at 0.003V.

- Press the play button to begin recording.

- Switch the machine to the on position momentarily and return it to the “off” position immediately after the rammer has been dropped, successive impacts of the rammer could damage the load cell or the rammer face. It is imperative that only one impact occur at a time and that it occur squarely on the load cell face.

- Realign the rammer for the next impact again this alignment will be approximately 35-45 degrees from the load cell face. Following the alignment steps outlined above.

- Switch the machine on for a single impact. Continue repeating rammer alignment and turning the machine on for a single impact on the load cell face until at least 3 impacts have been recorded.

    - Note the macro to handle data processing can handle a maximum of 5 impacts.

- Follow the same steps presented in the segment about saving and importing the data into excel.

Compliance Energy Processing

- On the keyboard of the laptop press the control key and the “r” at the same time. This begins the automated data processing of the compressive energy.

- The table generated from this data displays the compressive energy from each of the impacts recorded. The variance of these values is directly related to accuracy of the rammer alignment by the user and thus not reported. The mean is reported and representative of the machine as long as proper care was taken by the operator to align the rammer properly before switching the device on. On the plot of the forces note the impact number of any erroneous impacts and remove them from the summary for the machine.

APPENDIX B
DATA RESULTS

Table B-1. T-180 Rammer Rotation Summary Statistics Per Machine

		Velocity (in/sec)			Kinetic Energy (ft-lb)		
Machine Number	Rammer Mass (lbs)	Mean	Median	Standard Deviation	Mean	Median	Standard Deviation
1	10.00	110.59	110.98	2.02	13.20	13.29	0.48
2	10.00	110.92	110.98	0.82	13.28	13.30	0.20
3	10.00	112.96	113.10	1.14	13.78	13.81	0.28
4	9.98	114.61	114.46	0.44	14.15	14.11	0.11
5	10.02	114.36	114.46	0.45	14.14	14.17	0.11
6	10.00	113.12	113.37	0.70	13.81	13.87	0.17
7	9.98	111.22	111.24	0.46	13.32	13.33	0.11
8	9.99	114.24	114.18	0.69	14.07	14.06	0.17
9	10.00	102.57	100.42	4.61	11.37	10.88	1.03
10	10.00	114.61	114.73	0.80	14.17	14.20	0.20
11	10.01	111.51	111.76	0.67	13.43	13.49	0.16
12	10.00	114.79	115.01	0.37	14.22	14.28	0.09
13	10.00	114.54	114.73	0.82	14.15	14.20	0.20
14	10.00	113.54	113.37	0.90	13.92	13.87	0.22
15	10.00	113.91	114.18	0.53	14.01	14.07	0.13
16	9.99	113.61	113.64	0.35	13.92	13.92	0.09
17	9.99	113.70	113.64	0.43	13.93	13.92	0.10
18	10.00	109.82	109.95	0.81	13.02	13.05	0.19
19	10.02	113.40	113.50	0.85	13.90	13.92	0.21
20	10.00	114.50	115.01	0.74	14.15	14.28	0.18
21	9.98	112.95	112.83	0.70	13.74	13.71	0.17
22	9.99	109.44	109.70	1.44	12.91	12.97	0.34
23	10.01	112.47	112.56	0.58	13.66	13.68	0.14
24	10.00	115.54	115.57	0.59	14.41	14.41	0.15
25	10.00	109.10	108.94	1.56	12.85	12.81	0.37
26	10.00	106.40	106.50	1.55	12.22	12.24	0.36
27	10.01	112.78	113.64	3.25	13.75	13.95	0.77
28	10.00	114.88	115.15	0.78	14.24	14.31	0.19
29	9.92	116.06	115.85	0.39	14.41	14.36	0.10
30	9.92	112.41	112.56	0.64	13.52	13.56	0.15

Table B-2. T-180B Base Compliance Summary Per Machine

Machine Number	Average Integral of Force^2 (lbs^2-sec)	Base Mounting	Compressive energy (ft-lbs)
1	3686.23	Direct to Concrete	12.29
5	3533.44	Direct to Concrete	11.78
6	3672.25	Direct to Concrete	12.24
7	3176.89	Aluminium Spacer	10.59
9	3260.51	Aluminium Spacer	10.87
10	3381.72	Aluminium Spacer	11.27
11	3104.20	Aluminium Spacer	10.35
12	3691.42	Aluminium Spacer	12.30
15	4213.78	Aluminium Spacer	14.05
16	3393.28	Steel Spacer	11.31
18	3491.33	Aluminium Spacer	11.64
19	3774.38	Steel Spacer	12.58
20	3863.64	Steel Spacer	12.88
21	3433.66	Aluminium Spacer	11.45
23	3934.11	Aluminium Spacer	13.11
24	2566.72	Aluminium Spacer	8.56
26	3492.05	Aluminium Spacer	11.64
27	3334.38	Aluminium Spacer	11.11
30	3465.89	Steel Spacer	11.55

Note: Does not include plywood base mounting.

Table B-4. Soil Pill Results and Associated Energies 6% Moisture

	6%				
	Test Number	Percent Water Content (%)	Dry Unit Weight (pcf)	Kinetic Energy (ft-lbs)	Compliance Energy (ft-lbs)
		ω	γ	KE	CE
Machine 1	1	5.7	134.0	13.20	12.29
	2	5.7	134.5	13.20	12.29
	3	5.9	133.1	13.20	12.29
	4	5.6	133.8	13.20	12.29
	5	5.8	133.0	13.20	12.29
	6	5.5	133.5	13.20	12.29
	7	5.7	133.8	13.20	12.29
	8	5.7	134.7	13.20	12.29
	9	5.8	133.8	13.20	12.29
	10	5.6	134.3	13.20	12.29
Machine 14	1	5.8	132.7	13.92	11.31
	2	5.9	132.7	13.92	11.31
	3	5.8	133.2	13.92	11.31
	4	5.7	133.3	13.92	11.31
	5	5.9	133.1	13.92	11.31
	6	6	133.2	13.92	11.31
	7	6	133.2	13.92	11.31
	8	5.9	133.2	13.92	11.31
	9	5.8	133.1	13.92	11.31
	10	6	132.7	13.92	11.31
Machine 13	1	6.2	134.5	14.15	12.58
	2	5.6	133.6	14.15	12.58
	3	5.9	133.6	14.15	12.58
	4	6.3	134.2	14.15	12.58
	5	6.1	133.5	14.15	12.58
	6	6.1	133.7	14.15	12.58
	7	5.8	133.6	14.15	12.58
	8	6.1	134.0	14.15	12.58
	9	5.8	133.6	14.15	12.58
	10	6.3	133.8	14.15	12.58

Table B-4. Continued.

	6% continued				
	Test Number	Percent Water Content (%)	Dry Unit Weight (pcf)	Kinetic Energy (ft-lbs)	Compliance Energy (ft-lbs)
		ω	γ	KE	CE
Machine 11	1	5.4	131.9	13.43	10.87
	2	5.6	132.5	13.43	10.87
	3	5.6	132.1	13.43	10.87
	4	5.7	132.4	13.43	10.87
	5	5.8	132.3	13.43	10.87
	6	5.5	132.5	13.43	10.87
	7	5.7	132.2	13.43	10.87
	8	5.6	132.3	13.43	10.87
	9	5.7	132.6	13.43	10.87
	10	5.7	133.0	13.43	10.87
Machine 20	1	6.2	133.1	14.15	10.35
	2	5.7	133	14.15	10.35
	3	6	133.3	14.15	10.35
	4	6.1	135.1	14.15	10.35
	5	6	133.3	14.15	10.35
	6				
	7				
	8				
	9				
	10				
Machine 27	1	5.9	132.67	13.75	11.55
	2	5.8	133.3	13.75	11.55
	3	5.8	132.04	13.75	11.55
	4	5.8	132.54	13.75	11.55
	5	5.9	132.5	13.75	11.55
	6	5.9	132.3	13.75	11.55
	7	5.8	133.3	13.75	11.55
	8	6	132.4	13.75	11.55
	9	6	132.9	13.75	11.55
	10	5.8	133.5	13.75	11.55

Note: Only five test results reported on Machine 20

Table B-5. Soil Pill Results and Associated Energies 7.5% Moisture

	7.5%				
	Test Number	Percent Water Content (%)	Dry Unit Weight (pcf)	Kinetic Energy (ft-lbs)	Compliance Energy (ft-lbs)
		ω	γ	KE	CE
Machine 1	1	7.0	134.4	13.20	12.29
	2	6.6	134.4	13.20	12.29
	3	6.4	135.1	13.20	12.29
	4	6.8	134.8	13.20	12.29
	5	6.7	134.7	13.20	12.29
	6	7.3	133.9	13.20	12.29
	7	7.4	133.7	13.20	12.29
	8	7.4	133.9	13.20	12.29
	9	7.2	134.2	13.20	12.29
	10	7.2	134.1	13.20	12.29
Machine 14	1	7.5	133.3	13.92	11.31
	2	7.5	133.2	13.92	11.31
	3	7.7	132.8	13.92	11.31
	4	7.6	133.1	13.92	11.31
	5	7.7	133.3	13.92	11.31
	6	7.6	133.2	13.92	11.31
	7	7.6	132.7	13.92	11.31
	8	7.6	133.1	13.92	11.31
	9	7.5	133.0	13.92	11.31
	10	7.8	132.5	13.92	11.31
Machine 13	1	7.4	133.1	14.15	12.58
	2	7.5	133.2	14.15	12.58
	3	7.5	133.0	14.15	12.58
	4	7.4	133.3	14.15	12.58
	5	7.5	133.3	14.15	12.58
	6	7.5	133.3	14.15	12.58
	7	7.5	133.2	14.15	12.58
	8	7.5	133.0	14.15	12.58
	9	7.5	133.4	14.15	12.58
	10	7.4	133.4	14.15	12.58

Table B-5. Continued.

	7.5% continued				
	Test Number	Percent Water Content (%)	Dry Unit Weight (pcf)	Kinetic Energy (ft-lbs)	Compliance Energy (ft-lbs)
		ω	γ	KE	CE
Machine 11	1	7.5	133.6	13.43	10.87
	2	7.7	133.4	13.43	10.87
	3	7.2	134.1	13.43	10.87
	4	7.2	134.0	13.43	10.87
	5	7.2	134.1	13.43	10.87
	6	7.1	134.5	13.43	10.87
	7	7.2	134.0	13.43	10.87
	8	7.1	134.5	13.43	10.87
	9	7.3	133.9	13.43	10.87
	10	7.3	134.3	13.43	10.87
Machine 27	1	7.3	133.42	13.75	11.55
	2	7.4	133.42	13.75	11.55
	3	7.5	133.18	13.75	11.55
	4	7.5	133.05	13.75	11.55
	5	7.5	133	13.75	11.55
	6	7.9	132.4	13.75	11.55
	7	7.5	132.6	13.75	11.55
	8	7.5	132.6	13.75	11.55
	9	7.3	133.1	13.75	11.55
	10	7.3	133.5	13.75	11.55
Machine 26	1	7.7	131.7	12.22	8.56
	2	7.6	131.8	12.22	8.56
	3	7.7	131.8	12.22	8.56
	4	7.7	131.7	12.22	8.56
	5	7.6	132	12.22	8.56
	6	8.2	131.2	12.22	8.56
	7	7.7	131.8	12.22	8.56
	8	7.4	131.2	12.22	8.56
	9	7.8	131.7	12.22	8.56
	10	7.7	131.7	12.22	8.56

Regression Analysis 6%: γ versus ω, KE, CE

The regression equation is
γ = 122 + 0.846 ω + 0.007 KE + 0.489 CE

55 cases used, 5 cases contain missing values

Predictor	Coef	SE Coef	T	P
Constant	122.496	3.501	34.99	0.000
ω	0.8462	0.5711	1.48	0.145
KE	0.0069	0.3192	0.02	0.983
CE	0.4892	0.1167	4.19	0.000

S = 0.602469 R-Sq = 33.5% R-Sq(adj) = 29.6%

Analysis of Variance

Source	DF	SS	MS	F	P
Regression	3	9.3455	3.1152	8.58	0.000
Residual Error	51	18.5114	0.3630		
Total	54	27.8569			

Source	DF	Seq SS
ω	1	2.7298
KE	1	0.2351
CE	1	6.3806

Unusual Observations

Obs	ω	γ	Fit	SE Fit	Residual	St Resid
8	5.70	134.700	133.422	0.166	1.278	2.21R
22	5.60	133.600	133.486	0.307	0.114	0.22 X
44	6.10	135.100	132.818	0.209	2.282	4.04R

R denotes an observation with a large standardized residual.
X denotes an observation whose X value gives it large leverage.

Regression Analysis 6%: γ standardized versus, ω standardized, KE standardized, CE standardized

```
The regression equation is
γ stdzd = - 0.071 + 0.235 ω stdzd + 0.004 KE stdzd + 0.572 CE stdzd


55 cases used, 5 cases contain missing values


Predictor      Coef  SE Coef      T      P
Constant   -0.0715   0.1152  -0.62  0.538
ω stdzd     0.2349   0.1586   1.48  0.145
KE stdzd    0.0037   0.1733   0.02  0.983
CE stdzd    0.5721   0.1364   4.19  0.000


S = 0.838813   R-Sq = 33.5%   R-Sq(adj) = 29.6%


Analysis of Variance

Source           DF       SS      MS     F      P
Regression        3  18.1160  6.0387  8.58  0.000
Residual Error   51  35.8840  0.7036
Total            54  54.0000


Source    DF   Seq SS
ω stdzd    1   5.2917
KE stdzd   1   0.4557
CE stdzd   1  12.3686


Unusual Observations

Obs  ω stdzd  γ stdzd     Fit  SE Fit  Residual  St Resid
  8    -0.68    2.086   0.307   0.232     1.779      2.21R
 22    -1.19    0.555   0.396   0.427     0.159      0.22 X
 44     1.32    2.643  -0.534   0.291     3.177      4.04R

R denotes an observation with a large standardized residual.
X denotes an observation whose X value gives it large leverage.
```

Regression Analysis7.5%: γ versus ω, KE, CE

The regression equation is
γ = 144 - 2.05 ω + 0.202 KE + 0.187 CE

Predictor	Coef	SE Coef	T	P
Constant	143.652	1.875	76.63	0.000
ω	-2.0540	0.2450	-8.38	0.000
KE	0.2019	0.1868	1.08	0.284
CE	0.1871	0.1001	1.87	0.067

S = 0.422038 R-Sq = 79.9% R-Sq(adj) = 78.8%

Analysis of Variance

Source	DF	SS	MS	F	P
Regression	3	39.704	13.235	74.30	0.000
Residual Error	56	9.975	0.178		
Total	59	49.679			

Source	DF	Seq SS
ω	1	32.937
KE	1	6.145
CE	1	0.622

Unusual Observations

Obs	ω	γ	Fit	SE Fit	Residual	St Resid
3	6.40	135.100	135.471	0.198	-0.371	-0.99 X
40	7.30	134.300	133.403	0.077	0.897	2.16R
56	8.20	131.200	130.878	0.189	0.322	0.85 X
58	7.40	131.200	132.521	0.137	-1.321	-3.31R

R denotes an observation with a large standardized residual.
X denotes an observation whose X value gives it large leverage.

Regression Analysis 7.5%: γ standardized, versus ω standardized, KE standardized, CE standardized

```
The regression equation is
γ stdzd = - 0.0012 - 0.679 ω stdzd + 0.152 KE stdzd + 0.293 CE stdzd


Predictor      Coef  SE Coef      T      P
Constant   -0.00121  0.05938  -0.02  0.984
ω stdzd    -0.67891  0.08097  -8.38  0.000
KE stdzd     0.1518   0.1405   1.08  0.284
CE stdzd     0.2931   0.1568   1.87  0.067


S = 0.459930   R-Sq = 79.9%   R-Sq(adj) = 78.8%


Analysis of Variance

Source          DF      SS      MS      F      P
Regression       3  47.154  15.718  74.30  0.000
Residual Error  56  11.846   0.212
Total           59  59.000


Source    DF  Seq SS
ω stdzd    1  39.117
KE stdzd   1   7.298
CE stdzd   1   0.739


Unusual Observations

Obs  ω stdzd  γ stdzd      Fit  SE Fit  Residual  St Resid
  3    -3.37   2.0564   2.4603  0.2157   -0.4039     -0.99 X
 40    -0.41   1.1846   0.2068  0.0844    0.9777      2.16R
 56     2.56  -2.1937  -2.5450  0.2062    0.3513      0.85 X
 58    -0.08  -2.1937  -0.7542  0.1488   -1.4395     -3.31R

R denotes an observation with a large standardized residual.
X denotes an observation whose X value gives it large leverage.
```

LIST OF REFERENCES

American Association of State Highway Transportation Officials (AASHTO). *AASHTO standard test methods*. "T 87-86 Dry Preparation of Disturbed Soil and Soil Aggregate Samples for Test"; "T 99-01 Moisture Density Relations of Soils Using a 2.5 kg (5.5 lb) Rammer and a 305 mm (12 in.) Drop"; "T 180-01 Moisture Density Relations of Soils Using a 4.54 kg (10 lb) Rammer and a 457 mm (18 in.) Drop"; "T 88 Particle Size Analysis of Soils."

American Society for Testing and Materials (ASTM). *ASTM standard test methods*. "D 2168-02a Calibration of Laboratory Mechanical Rammer Soil Compactors."

Clinch, J. R. (2006). "Soil compaction: a comparison of standard Proctor and modified Proctor tests." Honors Thesis. Department of Civil and Coastal Engineering, University of Florida, Gainesville.

Das, B. M. (2002). *Principles of geotechnical engineering*. 5th ed. Pacific Grove: Brooks/Cole, 100–117.

Dubose, L. A. (1952). "Evaluating taylor marl clay for improved use in subgrades." *Texas Engineering Experiment Station Research Report 35*. Texas A&M College, Texas.

Halliday, D., Resnick, R., and Walker, J. (2000). "Fundamentals of physics." 6th ed. New York: Wiley.

Palacios, A. (1977). "The theory and measurement of energy transfer during standard penetration test sampling." Ph.D. Dissertation. Department of Civil Engineering, University of Florida, Gainesville, Fl.

Proctor, R.R. (1933). "Description of field and laboratory methods." *Engineering News Record*. September 7, 286–289.

Ray, P. N., and Chapman, T. G. (1954). "British standard compaction test for soils: study of some factors affecting test results**."** *Geotechnique*. Vol. 4 (4), December, 169–177.

Sebesta, S., and Liu, W. (2007). "Improving calibration and quality control of Proctor-style laboratory compaction*."* *Transportation Research Board,* July.

Sherwood, P. T. (1970). "The reproducibility of the results of soil classification and compaction tests**."** *RRL LR 339*. Road Research Laboratory, 27–37.

Texas Department of Transportation (TexDOT). "Laboratory Compaction Characteristics and Moisture Density Relationship of Base Materials." *TexDOT-113-E*.

BIOGRAPHICAL SKETCH

Keith Beriswill was born in Lakeland, Florida. He lives with his parents and two siblings. Keith has been involved in his local church and youth ministry and was active in other outside activities that have model his life. He was an active member of the Boy Scouts of America achieving the highest rank of Eagle Scout in 2001.

Keith graduated from George Jenkins High School in Lakeland, Florida in 2002 and was accepted to enter the University of Central Florida the following fall where he studied and graduated with his BSCE, majoring in civil engineering in the spring 2007. His desire for further education led him to the University of Florida to pursue a Master of Engineering degree with a focus in geotechnical engineering.

Upon graduation, Keith will be entering into industry in the field of geotechnical engineering, where he will be working in the area of dams and water resources.